

REFERENCE USE ONLY

FAA-75-14
REPORT NO. FAA-RD-76-44

THE DEVELOPMENT OF AN ATCRBS
MONOPULSE MEASUREMENT CAPABILITY
AT THE TRANSPORTATION SYSTEMS CENTER,
FISCAL YEAR 1974

Robert M. Weigand

U.S. DEPARTMENT OF TRANSPORTATION
Transportation Systems Center
Kendall Square
Cambridge MA 02142



MAY 1976
INTERIM REPORT

DOCUMENT IS AVAILABLE TO THE PUBLIC
THROUGH THE NATIONAL TECHNICAL
INFORMATION SERVICE, SPRINGFIELD,
VIRGINIA 22161

Prepared for

U.S. DEPARTMENT OF TRANSPORTATION
FEDERAL AVIATION ADMINISTRATION
Systems Research and Development Service
Washington DC 20591

NOTICE

This document is disseminated under the sponsorship of the Department of Transportation in the interest of information exchange. The United States Government assumes no liability for its contents or use thereof.

NOTICE

The United States Government does not endorse products or manufacturers. Trade or manufacturers' names appear herein solely because they are considered essential to the object of this report.

1. Report No. FAA-RD-76-44		2. Government Accession No.		3. Recipient's Catalog No.	
4. Title and Subtitle THE DEVELOPMENT OF AN ATRCBS MONOPULSE MEASUREMENT CAPABILITY AT THE TRANSPORTATION SYSTEMS CENTER, FISCAL YEAR 1974				5. Report Date May 1976	
				6. Performing Organization Code	
7. Author(s) Robert M. Weigand				8. Performing Organization Report No. DOT-TSC-FAA-75-14	
9. Performing Organization Name and Address U.S. Department of Transportation Transportation Systems Center Kendall Square Cambridge MA 02142				10. Work Unit No. (TRAIS) FA519/R6112	
				11. Contract or Grant No.	
12. Sponsoring Agency Name and Address U.S. Department of Transportation Federal Aviation Administration Systems Research and Development Service Washington DC 20591				13. Type of Report and Period Covered Interim Report Fiscal Year 1974	
				14. Sponsoring Agency Code	
15. Supplementary Notes					
16. Abstract To demonstrate the potential of monopulse in the ATC environment an experimental facility has been established at TSC. The components of the facility are described and a functional description of the TSC monopulse receiver used in the first year's effort is presented. An error analysis defines the measurement accuracy possible in using the TSC monopulse receiver. Results of two experiments are also presented in this report. The first shows the monopulse accuracy degradation due to receiver noise for targets at an equivalent of a 200 nmi range; the second graphically demonstrates the effect of interference on target location capability. Finally, recommendations for a follow-on activity are presented.					
17. Key Words ATCRBS Monopulse Beacon			18. Distribution Statement DOCUMENT IS AVAILABLE TO THE PUBLIC THROUGH THE NATIONAL TECHNICAL INFORMATION SERVICE, SPRINGFIELD, VIRGINIA 22161		
19. Security Classif. (of this report) Unclassified		20. Security Classif. (of this page) Unclassified		21. No. of Pages 58	22. Price

PREFACE

The work described in this report was carried out in the Radar and Navigation Branch at the Transportation Systems Center for the Systems Research and Development Service (FAA-SRDS), Department of Transportation. The objective of this effort was to establish an in-house experimental facility for evaluating the use of monopulse azimuth location in the air traffic control radar beacon system.

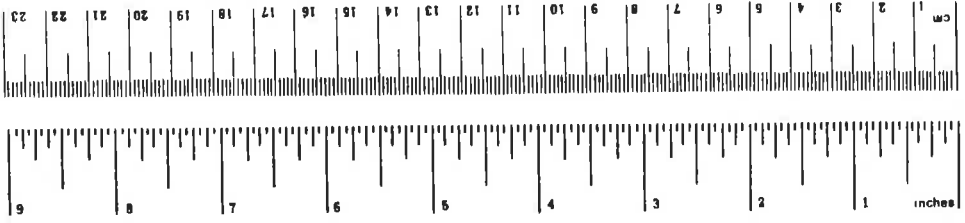
The author wishes to acknowledge the support of Mr. Donald A. Jenkins and Mr. Martin Natchipolsky of the Systems Research and Development Service, Federal Aviation Administration.

In the course of developing and testing the TSC monopulse receiver, the author acknowledges the contribution of Mr. Robert Rudis who designed the single hit processor and Mr. Charles Dunne who assisted in fabricating the receiver and making monopulse measurements.

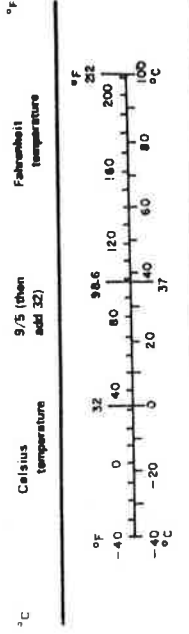
The author further acknowledges the support and encouragement of Dr. Benard Kulke and Mr. George G. Haroules. Art, technical typing, and editorial services were provided by the Raytheon Service Company, Ronald Karr, Technical Editor.

METRIC CONVERSION FACTORS

Approximate Conversions to Metric Measures				Approximate Conversions from Metric Measures			
Symbol	When You Know	Multiply by	To Find	Symbol	When You Know	Multiply by	To Find
LENGTH							
in	inches	2.5	centimeters	mm	millimeters	0.04	inches
ft	feet	30	centimeters	cm	centimeters	0.4	inches
yd	yards	0.9	meters	m	meters	3.3	feet
mi	miles	1.6	kilometers	km	kilometers	0.6	miles
AREA							
in ²	square inches	6.5	square centimeters	cm ²	square centimeters	0.16	square inches
ft ²	square feet	0.09	square meters	m ²	square meters	1.2	square yards
yd ²	square yards	0.8	square meters	km ²	square kilometers	0.4	square miles
mi ²	square miles	2.6	square kilometers	ha	hectares (10,000 m ²)	2.5	square miles
MASS (weight)							
oz	ounces	28	grams	g	grams	0.035	ounces
lb	pounds	0.45	kilograms	kg	kilograms	2.2	pounds
	short tons (2000 lb)	0.9	tonnes	t	tonnes (1000 kg)	1.1	short tons
VOLUME							
teaspoons	teaspoons	5	milliliters	ml	milliliters	0.03	fluid ounces
tablespoons	tablespoons	15	milliliters	ml	liters	2.1	pints
fl oz	fluid ounces	30	milliliters	ml	liters	1.06	quarts
c	cups	0.24	liters	l	liters	0.26	gallons
pt	pints	0.47	liters	l	cubic meters	35	cubic feet
qt	quarts	0.95	liters	m ³	cubic meters	1.3	cubic yards
gal	gallons	3.8	liters	m ³			
ft ³	cubic feet	0.03	cubic meters	m ³			
yd ³	cubic yards	0.76	cubic meters	m ³			
TEMPERATURE (exact)							
°F	Fahrenheit temperature	5/9 (after subtracting 32)	Celsius temperature	°C	Celsius temperature	9/5 (then add 32)	Fahrenheit temperature



TEMPERATURE (exact)



CONTENTS

<u>Section</u>	<u>Page</u>
1. INTRODUCTION.....	1
2. TSC MONOPULSE EXPERIMENTAL FACILITY.....	3
3. FUNCTIONAL DESCRIPTION OF THE TSC MONOPULSE SYSTEM...	8
3.1 Monopulse Antenna.....	8
3.2 RF Cabling.....	10
3.3 Monopulse Receiver.....	11
3.3.1 Diplexer.....	11
3.3.2 Mixer Preamplifier and Local Oscillator..	13
3.3.3 Logarithmic IF Amplifiers.....	13
3.4 Sampling.....	17
3.4.1 Single Reply Sampling.....	17
3.4.2 Boxcar Integrator.....	18
3.5 Data Recording and Calibration.....	19
4. ERROR ANALYSIS FOR LOG MONOPULSE RECEIVER.....	23
4.1 Receiver Sensitivity.....	23
4.2 Receiver Gain Mismatch.....	26
4.3 Quantization Errors.....	30
4.4 Pedestal Synchro Errors.....	31
5. MONOPULSE ACCURACY AT LOW SIGNAL LEVELS.....	33
6. MONOPULSE ERRORS DUE TO INTERFERING SIGNALS.....	37
6.1 Interference Test Bed.....	37
6.2 Data Format.....	39
6.3 Interpretation of Recorded Interference Data....	39
6.4 Results of Inverting Interference Data.....	44
7. RECOMMENDATION FOR FOLLOW-ON EFFORT.....	50
REFERENCES.....	52

LIST OF ILLUSTRATIONS

<u>Figure</u>	<u>Page</u>
1. TSC Monopulse Experimental Facility, FY '74.....	4
2. Interrogator Antenna.....	5
3. Monopulse System Components in 11th Floor Beacon Laboratory (a) Antenna Azimuth Control and Slaved Chart Recorder (b) Monopulse Receiver and UPX-6 Transmitter.....	6
4. Two Remote Fixed Transponder Sites (a) M.I.T. (b) Waltham.....	7
5. Monopulse Receiver - Block Diagram.....	9
6. Transfer Characteristic of a Log Amplifier.....	14
7. Σ and Δ Channel Output Responses.....	20
8. Monopulse Error Curve.....	22
9. Ratio of Off-Axis Error to On-Axis Error.....	27
10. Error Sources in Monopulse Azimuth Measurement.....	28
11. Measured Log Monopulse Receiver Performance, S/N=20dB.	35
12. Test Bed for Interference Measurements.....	38
13. Calibration Curves for S/I=2.8dB.....	40
14. Log Monopulse Response, S/I=2.8dB.....	41
15. Log Monopulse Response, S/I=5.6dB.....	41
16. Log Monopulse Response, S/I=9.2dB.....	42
17. Log Monopulse Response, S/I=15.6dB.....	42
18. Indicated Target Locations Due to Coherent Interference	43
19. Uncertainty in Aircraft Azimuth, S/I=15.6dB.....	45
20. Uncertainty in Aircraft Azimuth, S/I=9.2dB.....	46
21. Uncertainty in Aircraft Azimuth, S/I=5.6dB.....	47

1. INTRODUCTION

The Air Traffic Control Radar Beacon System (ATCRBS) is becoming the primary means of aircraft surveillance. Present air traffic control (ATC) beacon interrogator/receivers use a sliding window processor to generate aircraft centermark estimates. The sliding window processor inherently requires a high interrogation rate for accurate centermarking. The increasing population of transponder equipped aircraft and interrogator sites combined with the required high interrogation rates may ultimately result in intolerable centermarking errors due to reduced round reliability and reply interference. These problems will be alleviated if the interrogation rate required to accurately centermark an aircraft can be reduced.

A monopulse processor has potential of providing accurate target centermarking with but a few interrogations.^{1,2} Ideally, all the information required to centermark the azimuth of an aircraft to a small fraction of an antenna beamwidth is available upon the reception of a single transponder reply. A calibrated monopulse receiver generates a signal, the error voltage, indicative of the differential azimuth of a reply from antenna boresight. The error voltage is translated to azimuth offset from antenna boresight and is added to the antenna boresight angle obtained from a pedestal shaft encoder to provide an aircraft centermark.

$$\theta_A = \theta_B + \theta_M \quad (1-1)$$

where

θ_A = azimuth of transponder equipped aircraft

θ_B = azimuth of antenna boresight derived from antenna pedestal shaft encoder at the time the transponder reply is received

θ_M = azimuth offset angle of transponder reply from antenna boresight derived from the monopulse error voltage

Under the non-ideal conditions of signal-to-noise ratio and reply interference that exist in ATCRBS, monopulse has potential of matching the accuracy of a sliding window processor while requiring a lower interrogation rate.

A program was initiated during Fiscal Year 1974 to evaluate experimentally the feasibility of using monopulse for aircraft azimuth centermarking in the ATC environment. During the first year a monopulse receiver was designed and built at TSC, and a second monopulse receiver and signal processor was specified and built under contract.

The receiver built at TSC has been used in preliminary measurements to define beacon monopulse accuracy at low signal-to-noise levels and to determine the effect of coherent interference on accuracy. The results of these measurements are contained in this report. The program is expected to lead to an experimental comparison of the performance of the monopulse and sliding window techniques of centermarking.

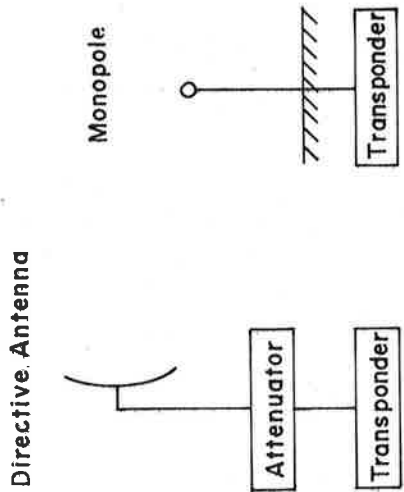
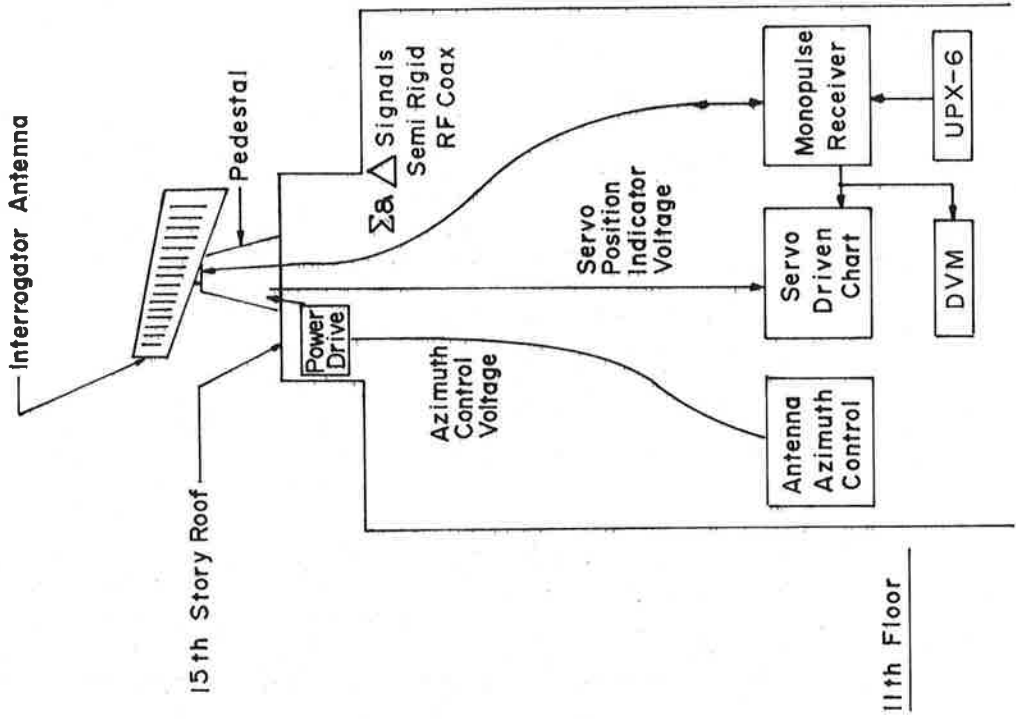
2. TSC MONOPULSE EXPERIMENTAL FACILITY

This section presents an overview of the facility developed to support the monopulse measurements made at TSC during Fiscal Year 1974. Figure 1 shows the location of the major components of the facility. The interrogator antenna, shown in Figure 2, is a planar array located above the 15th story roof of Building #1 at TSC. The antenna pedestal is servo-controlled, which allows the antenna to be either rotated or positioned to any desired azimuth. The pedestal controls are located in the 11th floor Beacon Laboratory. Within the pedestal a gear train is employed to develop 1:1 and 36:1 positional servo signals. These servo signals may be used to slave an antenna pattern recorder to antenna azimuth. Figure 3 shows the antenna control panel and slaved chart recorder.

Beacon system interrogations and replies are transmitted and received by the monopulse antenna. The sum (Σ) and difference (Δ) channel signals are passed through a dual channel rotary joint inside the pedestal to a pair of semi-rigid coaxial cables running to the 11th floor. The cable run is approximately 190 feet. These received signals are amplified in a pair of closely matched receiver channels. The output of the receiver is monitored on a digital voltmeter or recorded in analog form on the chart recorder slaved to antenna azimuth.

In Fiscal Year 1974 a UPX-6 transmitter/receiver was used for generating interrogation signals. Figure 3 shows the monopulse receiver with the UPX-6 transmitter/receiver at the bottom of the right hand rack.

For the beacon experiments TSC has established three remote transponder sites. These serve as fixed targets of known azimuth and range. The use of fixed targets permits certain data sets to be taken repeatedly while varying interesting system parameters. These targets also constitute a diagnostic tool for receiver check-out. Figure 4 shows two of the remote fixed transponder sites. At the Waltham transponder site either a directional antenna or omnidirectional antenna may be connected to the transponder.



Typical Fixed Remote Transponder Sites

TSC Building#1 Interrogator Site

Figure 1. TSC Monopulse Experimental Facility, FY '74

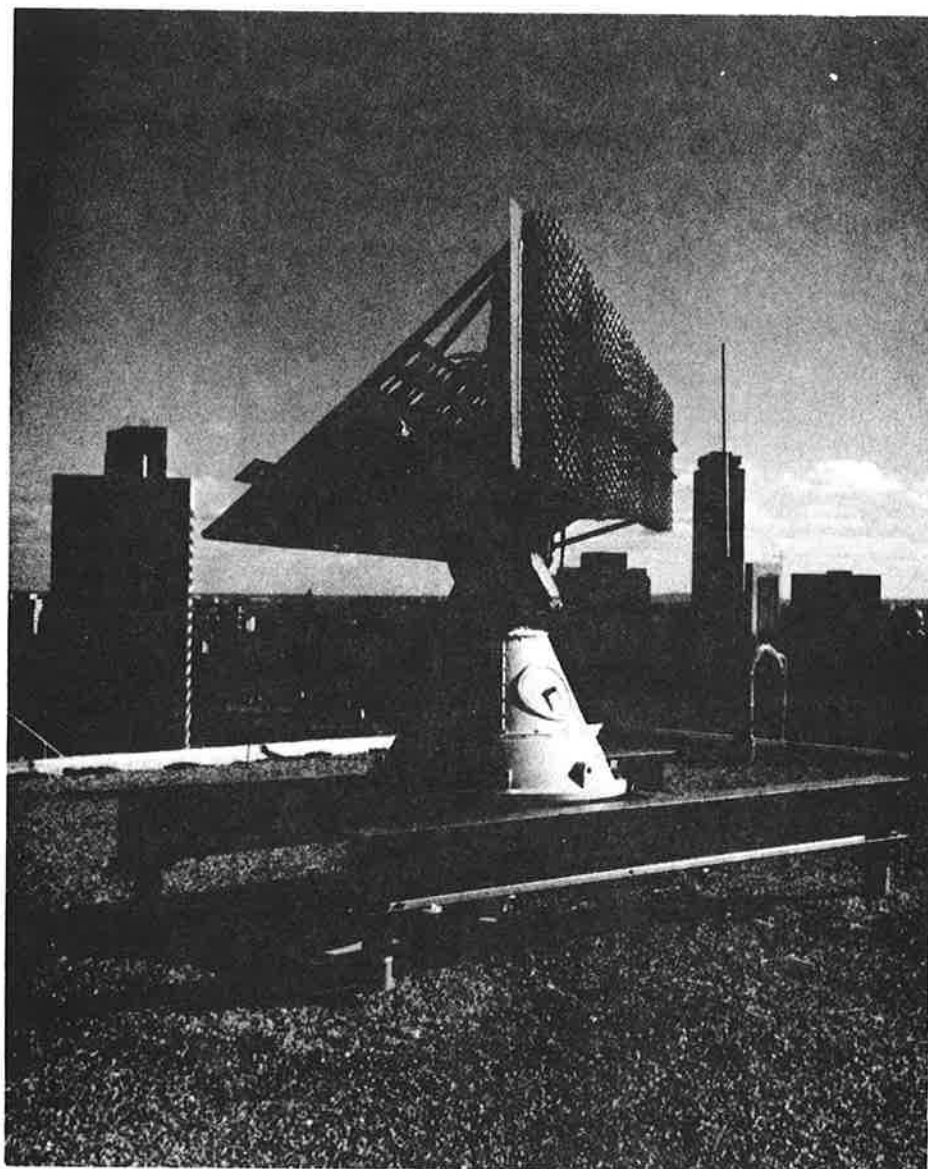
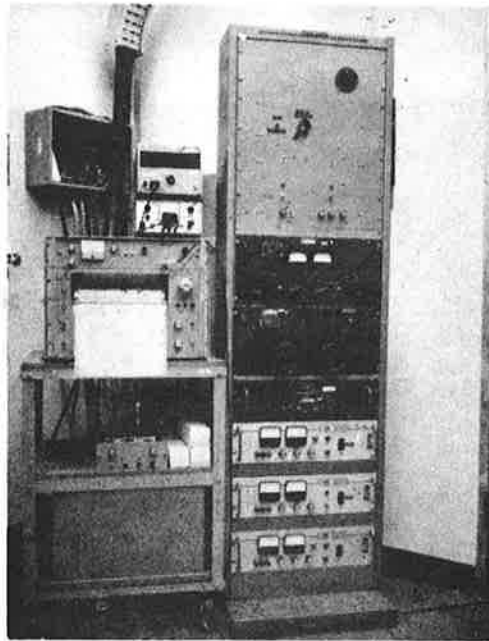
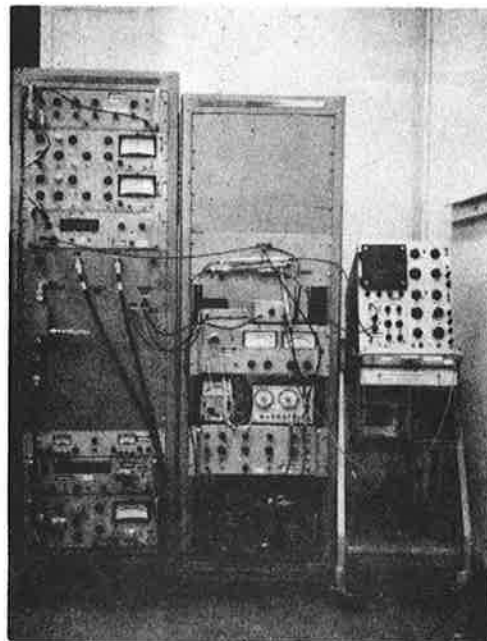


Figure 2. Interrogator Antenna

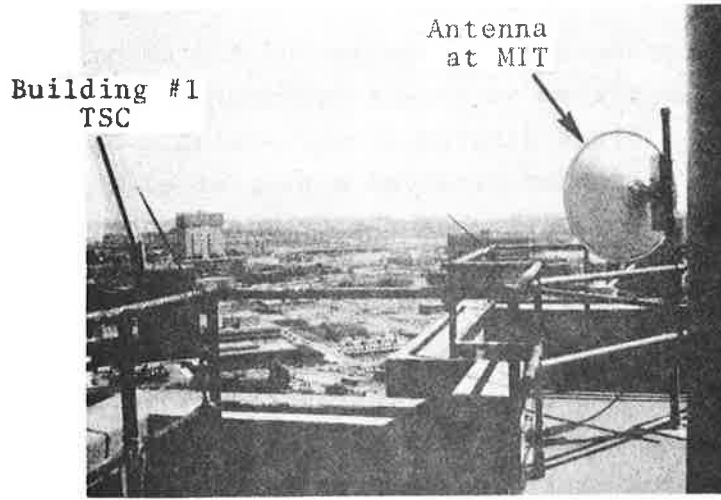


(a)

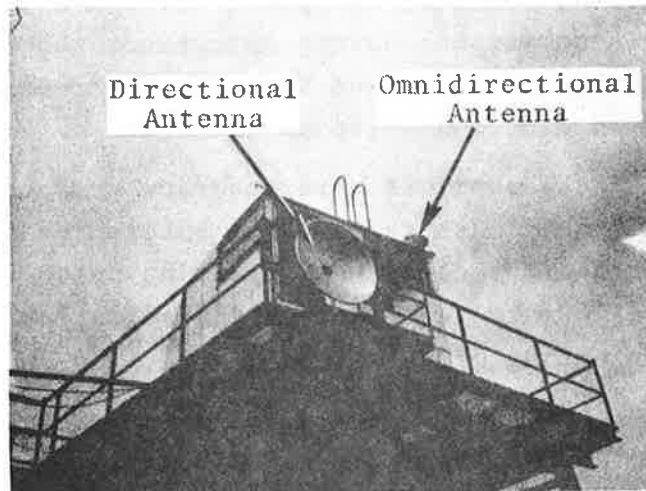


(b)

Figure 3. Monopulse System Components in 11th Floor Beacon Laboratory (a) Antenna Azimuth Control and Slaved Chart Recorder (b) Monopulse Receiver and UPX-6 Transmitter



(a)



(b)

Figure 4. Two Remote Fixed Transponder Sites (a) M.I.T. (b) Waltham

3. FUNCTIONAL DESCRIPTION OF THE TSC MONOPULSE SYSTEM

This section presents a description of the major components of the TSC monopulse system as it was configured in Fiscal Year 1974. Figure 5 is a block diagram of the system. Signals received from an airborne transponder produced a pair of voltages at a monopulse antenna output indicative of the azimuth offset of a reply from antenna boresight. Two identical receiver channels raised the signals to a level and into a form in which the monopulse off-boresight azimuth angle of a received signal could be readily determined. Only the received F_2 reply pulse amplitude was used for the monopulse measurements. Two distinct sampling devices were used to sample the log amplifier outputs at the appropriate moment in time and hold a replica of the pulse amplitude as a DC voltage for recording or display. A single hit sampler completed late in the year was used in experiments requiring the recording of data from individual transponder replies. This sampler was used to develop the error statistics of monopulse operation at low signal-to-noise ratios. A commercial boxcar integrator requiring a minimum interrogation rate of 50/second was used for recording the effect of interference on monopulse operation.

The outputs of the samplers were recorded on a chart recorder slaved to the antenna azimuth servo. The entire receiver was calibrated through the chart recorder by injecting pulse signals of known amplitude ratio into the receiver and adjusting the receiver gain for correct plotting of the signals.

3.1 MONOPULSE ANTENNA

The antenna currently in use at TSC is a planar array consisting of 32 element pairs arranged horizontally on a ground plane 5.6 meters long and 0.8 meters high. Each vertical pair is driven by one of 32 outputs of a Butler matrix. A Taylor amplitude distribution provides -27dB sidelobes. Two inputs to the Butler matrix provide fan beams squinted ± 1.6 degrees about boresight. Each fan beam has an azimuth beamwidth of 5° and an elevation beamwidth of 35° . The antenna has been tilted upward on its pedestal with its

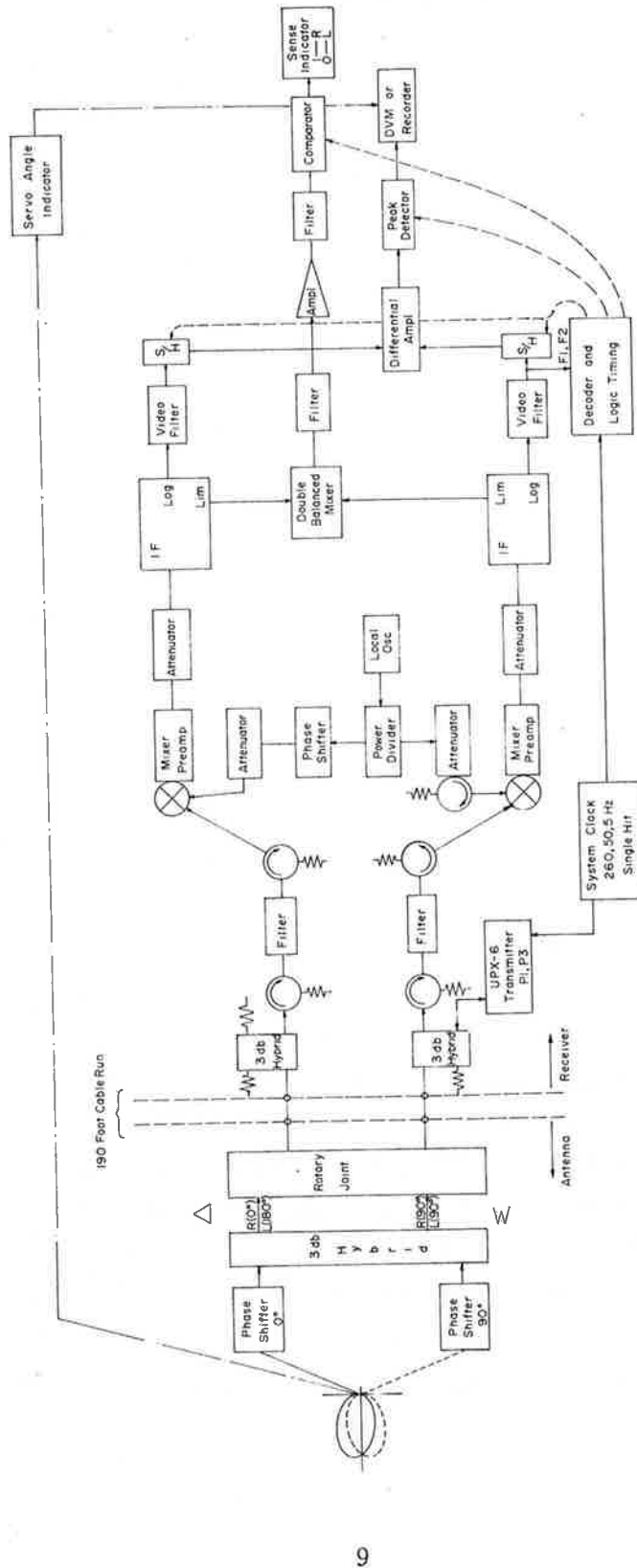


Figure 5. Monopulse Receiver - Block Diagram

axis 10° above the horizon in order to reduce reflections from the roof.

To form the desired sum and difference pattern voltages the two squinted beam outputs have to be combined as shown in Figure 5. The phase of one squinted beam is delayed 90° and combined with the other squinted beam in a 3dB comparator hybrid. The outputs of the comparator hybrid are the sum (Σ) and the difference (Δ) of the two squinted beams. The measured Σ pattern antenna gain at the output of the hybrid is 15.8dB, and the Σ pattern half power beamwidth is 4.7 degrees.

Phase errors occurring before the hybrid constitute pre-comparator phase errors. These impact on monopulse null depth and boresight shift.³ Operationally it has been determined that the phase shifter preceeding the Σ and Δ forming hybrid requires occasional adjustment to compensate for thermal line length changes in the antenna.

3.2 RF CABLING

The Σ and Δ signals formed in the hybrid have to be conducted through the pedestal and down a cable run of approximately 190 feet to the monopulse receiver on the 11th floor. The insertion loss of the cable run must be minimized to retain system sensitivity. Differential loss between the Σ and Δ cable runs has the effect of causing errors in measuring the magnitude of the monopulse off-boresight azimuth angle. Differential loss in the cabling should be held to less than 0.1dB. Post-comparator phase between Σ and Δ signals is used by the receiver to recover the directional sense of a reply. When a reply originates from right of boresight, Σ and Δ voltages are in phase; when a reply originates from left of boresight, these voltages are 180° out of phase. The differential phase shift through the cable run should be kept to well below 10° .

The first component of the cable run following the hybrid comparator is a dual channel rotary joint required for the free

rotation of the antenna. The measured loss through the rotary joint is less than 0.05dB and the measured differential phase between two channels is less than ± 0.5 degrees.

One hundred and seventy-five feet of the rf cable run from the roof to the Beacon Laboratory employs 7/8-inch semi-rigid cables having a foamed polyethylene dielectric. The total loss through these cables is 3.9dB. Interconnection between the semi-rigid cable and the monopulse receiver is made using 13 foot lengths of RG214 flexible cable. The loss due to the RG214 cables is 0.9dB.

3.3 MONOPULSE RECEIVER

In an azimuth monopulse system the receiver consists of two identical channels. Each channel contains a diplexer, a mixer-pre-amplifier and a log amplifier. A diplexer permits the 1030 MHz interrogation signals from the UPX-6 to be coupled to the Σ signal line for transmission over the antenna Σ pattern. The diplexer isolates the sensitive receiver from the high power transmitted signal. A mixer-preamplifier down-converts the received 1090 MHz reply signal to 60 MHz and provides low noise amplification. After preamplification, the signal enters a logarithmic IF amplifier with two outputs. The log amplifier generates a detected video signal with an amplitude equal to the log of the incoming signal pulse amplitude. Subtraction of the outputs of the two log amplifiers provides the required Δ/Σ ratio for determining magnitude of the azimuth offset of a reply from antenna boresight. Since a video signal cannot preserve the phase information of the received signal, a limiter output provides a replica of the phase of the incoming signal. A phase differential of 0° or 180° between the Σ and Δ channel limiter outputs provides the directional sense of the reply as originating from right or left of boresight.

3.3.1. Diplexer

The diplexer for each channel consists of a 3dB hybrid, a narrow bandpass filter, and a pair of circulators, as shown in Figure 5. A hybrid was chosen as the means of coupling the

monopulse receiver and the conventional transmitter/receiver (UPX-6 or TPX-42) to the Σ signal line. This approach permits the monopulse receiver to receive signals without affecting the normal operating performance of the conventional transmitter/receiver. This permits simultaneous measurements to be made with both receiver types. A hybrid in the Δ channel permits the P_2 pulse to be transmitted over the difference pattern for ISLS implementation.

Two disadvantages arise from use of 3dB hybrids. Half of the transmitter power is terminated in one of the outputs of the hybrid. This is not a severe penalty, since the full available power of the transmitter is not required. A second disadvantage, a reduction in sensitivity by 3dB, results from splitting the received power between monopulse receiver and TPX-42 or UPX-6. This affects the accuracy with which distant transponders can be located. For experimental purposes this loss is justified to permit parallel processing. Should monopulse be adapted for ATCRBS and a dedicated transmitter be combined with the receiver, most of the 3dB loss would be eliminated by combining transmitter and receiver through filters. This is the method by which transmit and receive signals are combined in present ATCRBS transmitter/receiver units.

The diplexers use bandpass filters centered to permit reception of the reply signal at 1090 ± 3 MHz. The rejection of the filters at the transmitter frequency of 1030 is greater than 60 dB. This prevents transmitter power from damaging the sensitive mixers. Since the bandpass filters are matched to the line impedance only in their bandpass region, a pair of circulators connected as isolators are positioned on either side of the filter. These serve to maintain a system impedance match around the filter. The isolation preceding the filter terminates power incident upon it due to reflections at the antenna or due to imperfect hybrid directivity. The circulator following the filter matches the mixer image frequency to prevent possible degradation of receiver noise figure. The average loss through the diplexer is 4.9dB at 1090 MHz. If filters were used to combine the signals, the expected loss should

be reduced to about 1.9dB.

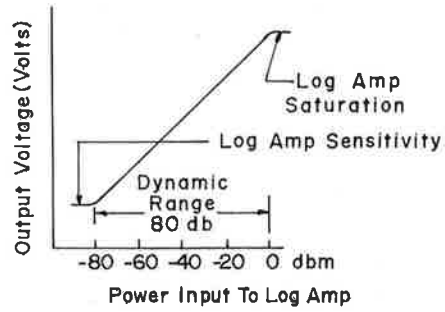
3.3.2 Mixer Preamplifier and Local Oscillator

Down conversion of the 1090 MHz Σ and Δ signals to 60 MHz and low noise amplification are accomplished using double balanced mixer-preamplifiers. The RF to IF gain of the mixers is 28dB with a 3dB bandwidth of 11 MHz. A common local oscillator drives both mixers to assure that the IF signals retain the phase relationship of the RF signals. A double balanced mixer provides superior RF to local oscillator isolation than a single balanced mixer. This is an important factor in assuring that Σ signal power does not reach the Δ signal mixer via the local oscillator at times when Σ to Δ ratio is large.

The adjustable phase shifter located between the local oscillator and Δ channel mixer compensates for fixed differential post-comparator phase shifts between the Σ and Δ channels due to factors such as unequal cable lengths. Its adjustment insures that replies from right of boresight are in-phase and replies from left of boresight have a phase differential of 180°. This adjustment is required only once for any set of interconnecting cables.

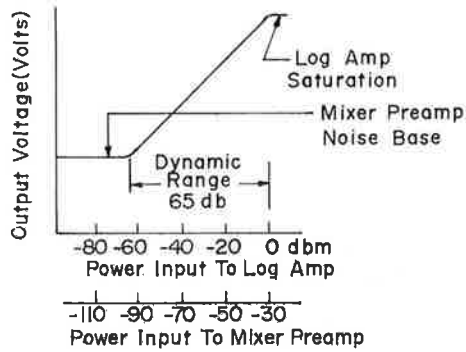
3.3.3 Logarithmic IF Amplifiers

The successive detection log IF amplifier used in the TSC monopulse receiver produces two distinct outputs derived from an incoming signal. The first output formed is a video signal with amplitude proportional to the log of the incoming signal power. The second output is a constant amplitude signal (limited) with phase related to the incoming signal. The transfer characteristic of the log output, as shown in Figure 6, is a straight line when the output in volts is plotted against the input in power over the useful dynamic range. Figure 6a shows the characteristic output of a typical log amplifier which has a dynamic range of 80dB. At the lower signal range the logging threshold defines the minimum signal required for the amplifier to form its log. At the upper signal range saturation limits the maximum signal which can be formed into a log output. The mixer preamplifier preceding the log amplifier should



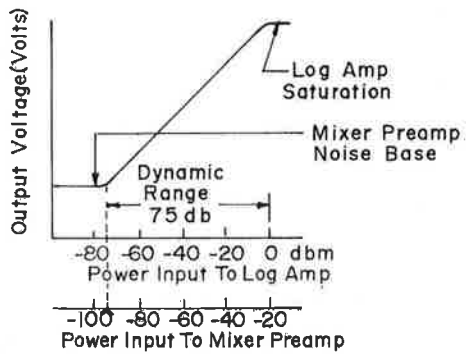
a

Log Amplifier
Characteristic



b

Log Amplifier
Preceded By
Mixer Preamp With
30 db RF-IF Gain
-95 dbm Input Noise
Level



c

Log Amplifier
Preceded By
Mixer Preamp With
20 db RF-IF Gain
-95 dbm Input Noise
Level

Figure 6. Transfer Characteristic of a Log Amplifier

have sufficient gain in order that the noise level of its output exceeds the logging threshold. This condition insures that all signals received above noise will be processed to form their log. If the mixer preamplifier gain is too great, the noise into the log amplifier will exceed the logging threshold by a considerable degree, resulting in a reduction in the dynamic range of the amplifier without any benefits of improved sensitivity. The high input noise level produces a d.c. voltage offset which masks the lower input power range, as shown in Figure 6b. A proper mixer preamplifier gain results in only a small reduction in dynamic range, as Figure 6c shows. The receiver built at TSC uses attenuators following the mixer preamplifier to provide gain matching.

The log output characteristic of the log amplifier is specified by the slope characteristic (k) in units of millivolts/decibel. This is a fixed characteristic of the amplifier. An offset adjustment in the log amplifier permits the d.c. component of the output voltage to be adjusted to meet a particular application. The log output is of the form

$$V_{out} = A + k \ 20 \log V_{in} \quad (3-1)$$

where

A = d.c. offset, adjustable

k = log slope characteristic, fixed

V_{in} = input signal, RMS voltage

The adjustable d.c. offset A permits the log amplifier output to be set to zero volts when the input is due solely to mixer preamplifier front-end noise. As a result, all signal voltages are read directly as signal above noise level. For a receiver sensitivity of -88dBm, A has a value of -k(88 dBm) volts. Therefore, the output of the log amplifier is

$$\begin{aligned} V_{out} &= -k(88 \text{ dBm}) + k \ 20 \log V_{in} & (3-2) \\ &= k (20 \log V_{in} - 88\text{dBm}) \end{aligned}$$

If the outputs of two log amplifiers with input voltages equal to V_{Σ} and V_{Δ} (the rms voltages from Σ and Δ channels) are subtracted, then

$$V_1 - V_2 = A_1 + k 20 \log V_{\Delta} - A_2 - k 20 \log V_{\Sigma} \quad (3-3)$$

If the d.c. offsets, A_1 , A_2 are equal

$$V_1 - V_2 = k 20 \log (V_{\Delta}/V_{\Sigma}) \quad (3-4)$$

The ratio V_{Δ}/V_{Σ} is the desired monopulse error curve. It is this ratio which indicates the magnitude of the azimuth offset of a reply from antenna boresight.

The video signals from the log amplifier are low pass filtered to improve matching of video bandwidth to transponder reply pulsewidth. For a reply pulsewidth of 450 nanoseconds, 1.5 MHz low pass filtering is used.

The signals from the Σ and Δ channel limiters have either 0° or 180° phase between them, depending on whether a reply originates from right or left of antenna boresight. A double balanced mixer is used to generate a positive or negative voltage, depending on the phase between the limiter signals. The output of a double balanced mixer has the form

$$v = b \cos (\Phi_{\Sigma} - \Phi_{\Delta}) \quad (3-5)$$

where

b = constant voltage amplitude, dependent on mixer conversion loss and limiter signal levels

Φ_{Σ} = phase of Σ channel voltage

Φ_{Δ} = phase of Δ channel voltage

If a reply originates from right of boresight, Σ and Δ are in phase and $V = +b$; but if the reply originates from left of boresight, Σ and Δ are 180° out of phase, resulting in $V = -b$. In the absence of interference the mixer will always generate either

+b or -b volts. In the presence of interfering signals the output will be reduced by an amount dependent on the cosine of the phase between Σ and Δ .

3.4 SAMPLING

The TSC monopulse system samples the outputs of the Σ and Δ channels and the output of the double balanced mixer in time coincidence with the reception of the F_2 transponder reply pulse. The sampling function extracts the useful information available at the time F_2 is received while rejecting extraneous signals occurring at other times. The sampled pulses are used to generate d.c. levels proportional to the sampled pulse amplitude for recording or display.

Two distinct sampling techniques were used in conjunction with the monopulse receiver. One sampler operates on a single reply; the other, a boxcar integrator, requires a minimum signal rate for proper operation.

3.4.1 Single Reply Sampling

A single hit sampler designed and built at TSC provides the capability of generating monopulse target estimates from a single interrogation. The components of the sampler are shown as part of the receiver block diagram, Figure 5.

Timing signals are generated by a bracket decoder activated by the system clock. The bracket decoder monitors a high impedance sample of the Σ channel log output. It generates a gate pulse when an F_2 pulse is received preceded by a properly spaced F_1 pulse. The bracket decoder ranges to the first valid target with proper F_1 to F_2 spacing at any range up to 200 miles after activation by the system clock. No further sampling gates are generated until a new clock signal is received.

The Σ and Δ log signals feed a pair of sample and hold circuits triggered by the sampling gate. The outputs feed into a differential amplifier to form the function

$$V = \alpha k 20 \log_{10} (V_{\Delta}/V_{\Sigma}) \quad (3-6)$$

where α includes loss due to the video filters and the gain of the differential amplifier. The output of the differential amplifier feeds a digital (A to D to A) peak detector. The peak detector holds each sample until it is cleared by the next interrogation clock pulse. The peak detector output is a d.c. voltage which can be read with a DVM or displayed on an analog chart recorder. The output polarity of the double balanced mixer is sensed by a comparator to determine whether a reply originated from right or left of boresight. The comparator output can also be read with a DVM or displayed on an analog chart recorder.

3.4.2 Boxcar Integrator

A commercial boxcar integrator was used preceding the completion of the single reply sampler. The boxcar time constant is set for 0.7 full scale in 7 samples. The post-detection smoothing this provides proved beneficial in recording certain data sets. The boxcar integrator functions only with fixed targets, since the sampling gate is derived by introducing a fixed delay after the system clock trigger. This fixed delay corresponds to the arrival of the F_2 pulse. The signal input to the boxcar is single ended, and an external differential amplifier of unity gain was therefore used for combining the log video outputs of the Σ and Δ channels.

The directional sense pulse which indicates whether the reply originates from right or left of the antenna axis is sampled by connecting the boxcar integrator to the double balanced mixer output in a separate scan past the desired target. The collection of data from separate scans past a target is only possible under conditions in which the returns from fixed targets are repeatable. The output of the boxcar integrator is a d.c. voltage proportional to the amplitude of the input video pulse. The output is usually fed to a calibrated chart recorder slaved to the antenna azimuth.

3.5 DATA RECORDING AND CALIBRATION

The outputs of the single reply sampler or boxcar integrator may be recorded using an analog chart recorder slaved to antenna azimuth or read directly using a DVM. The chart recorder scale factors provide for $\pm 180^\circ$, $\pm 30^\circ$, or $\pm 5^\circ$ full scale. An angle offset may be used to align the 0° mark of the chart paper to the azimuth of any fixed target. As the antenna rotates away from the target azimuth, the chart paper is driven in the proper scaled angular increments. Once the chart position of 0° is set, all patterns are indexed to that azimuth. The sampled output of the log amplifiers is recorded on chart paper having a 60dB logarithmic scale.

Adjustment of recorder gain permits incoming signals to be recorded in the proper log increments on the chart paper. A calibrated pulse signal at a peak power level of -28dBm is injected into the Σ channel while no signal is injected into the Δ channel. Recorder gain is adjusted to provide full scale recorder deflection of 60dB for this condition. At -28dBm the signal is 60dB above the -88dBm receiver noise level. Consequently, the chart paper is calibrated logarithmically from -28dBm to -88dBm. The calibration throughout the 60dB range can be verified by reducing the signal in fixed log increments and checking that the recorder properly tracks the signal levels. The DVM has a derived calibration based on the d.c. voltage required for full scale deflection of the recorder.

If only the Σ antenna signal feeds the receiver while the Δ antenna signal is terminated, a recording of the one-way Σ antenna pattern results. Similarly, if the Δ antenna signal feeds the receiver while the Σ antenna signal is terminated, a recording of the one-way Δ antenna pattern results. Figure 7 shows the result of scanning through a fixed transponder twice while individual Σ and Δ channel signals were recorded. The log error curve is recorded when both Σ and Δ signals are simultaneously connected to the receiver. In this case the bottom of the chart refers to $\Delta/\Sigma = 1$ (0db)

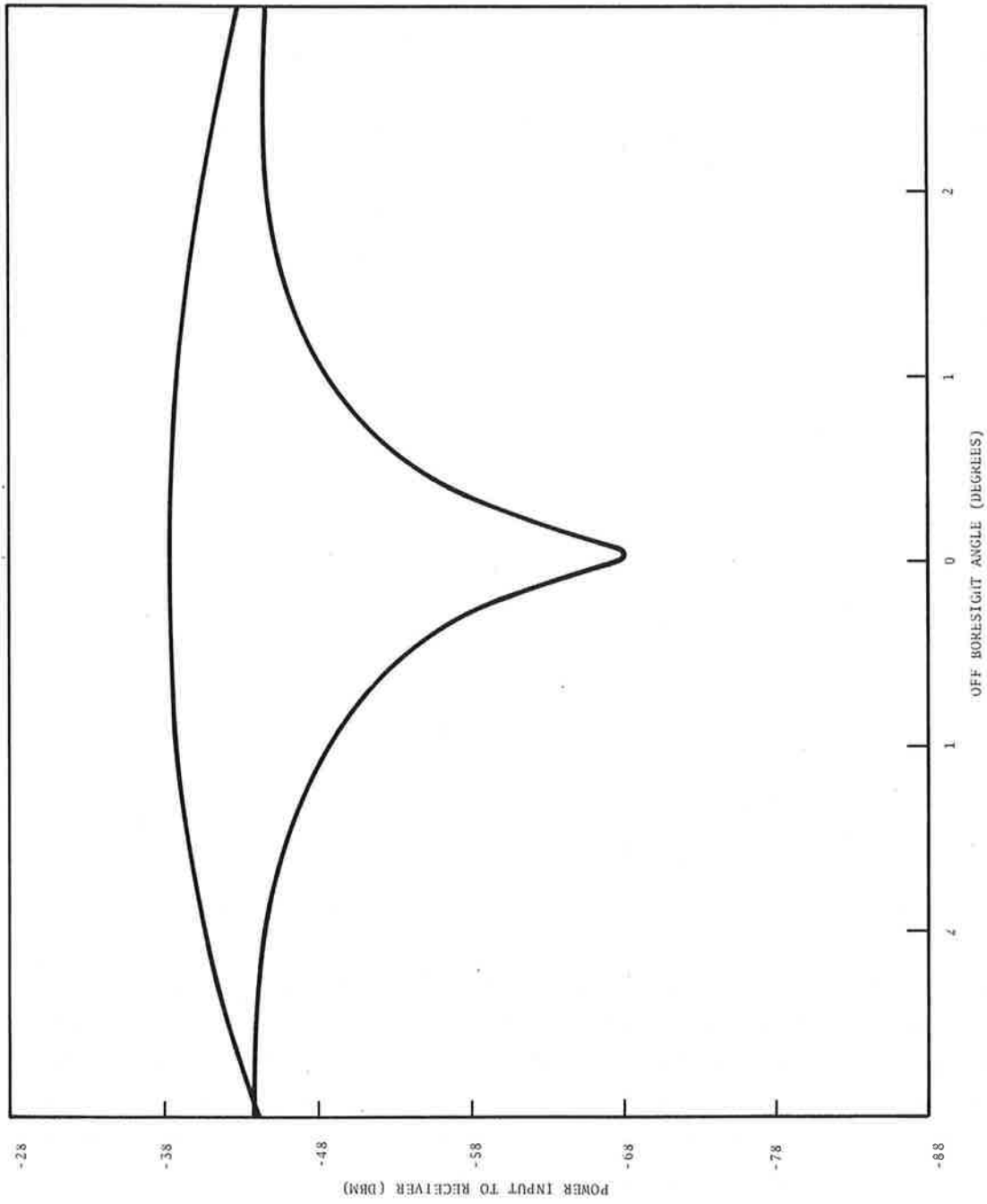


Figure 7. Σ and Δ Channel Output Responses

and the scale up from the chart bottom reads $(\log \Delta - \log \Sigma)$ in db below unity. When measurements are made in the presence of interference Δ/Σ can exceed unity. To permit these values to be plotted clearly, an offset is introduced between the processor output and the recorder input. The offset permits $\Delta/\Sigma=1$ (0dB) to be plotted 20dB above the chart bottom. It then becomes possible to plot values of $\Delta/\Sigma=.01$ (-40dB) to $\Delta/\Sigma = 10$ (20dB) on the chart. An example of an error curve for a target without interference is shown in Figure 8.

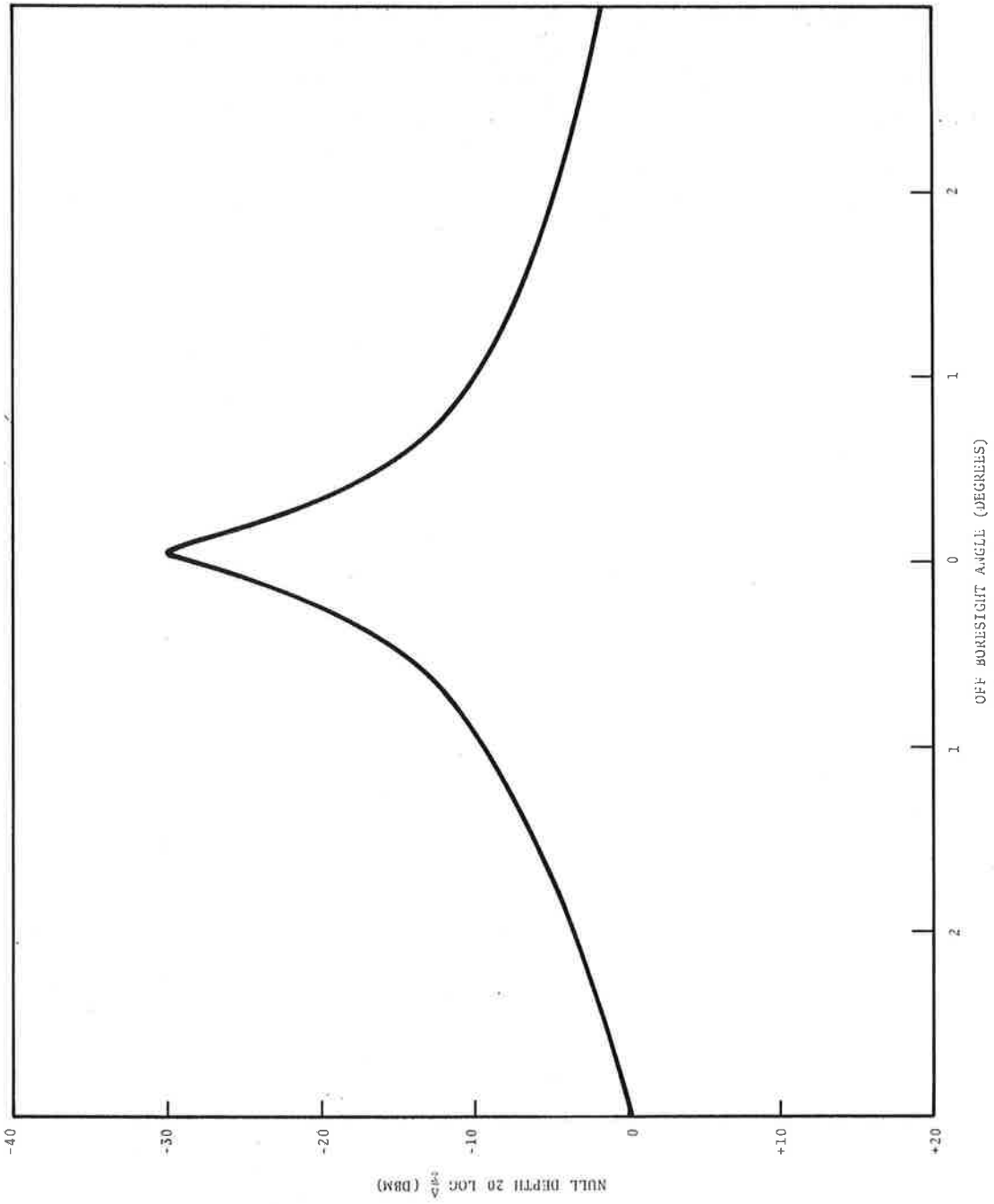


Figure 8. Monopulse Error Curve

4. ERROR ANALYSIS FOR LOG MONOPULSE RECEIVER

This section identifies error sources encountered in making monopulse azimuth measurements and provides quantitative results applicable to the TSC monopulse receiver. The sources considered in this section are those due to receiver sensitivity, channel gain tracking errors, quantization and pedestal synchro backlash. Errors due to interfering signals are considered in Section 6.

4.1 RECEIVER SENSITIVITY

The transponder reply signal to receiver noise ratio limits the accuracy with which a monopulse receiver can centermark the position of distant aircraft at ranges approaching the maximum operating range of 200 nautical miles. In this section the S/N expected from distant targets is calculated, and from this the magnitude of azimuth measurement error is derived. The results of this section are verified by experiments described in Section 5.

Transponders used on commercial aircraft transmit as much as 500 watts of peak power. The typical peak power of transponders used in general aviation is 200 watts. The received power from such a transponder when using the antenna and receiver at TSC at an intermediate range of 50 nautical miles is given by

$$P_R = \frac{P_T G_T G_R \lambda^2 L}{16 \pi^2 R^2} \quad (4-1)$$

where

P_R = peak power at input to receiver

P_T = peak power output of transponder, 200 watts

G_T = transponder antenna gain, 0dB(1x)

G_R = receiver antenna gain, Σ pattern, 15.8dB (38x)

λ = wavelength, 0.9 feet

L = cable loss, -4.8dB (0.33)

R = range, 50 nmi x 6080.2 ft/nmi

$$P_R = 1.39 \times 10^{-10} \text{ watts} = -68.6 \text{ dBm}$$

The mixer preamplifier noise power referred back to the input of the receiver diplexer is measured as approximately -88dBm. Therefore, the signal-to-noise (S/N) of replies from a 200-watt transponder 50 nmi distant is approximately 20dB on boresight. The signal-to-noise ratio in a beacon system decreases as the square of aircraft range. If a transponder-equipped aircraft were located at the maximum beacon range of 200 nmi, the transponder reply would be reduced by an additional 12.0dB, with an equal reduction in signal-to-noise.

Fortunately, significant improvement in signal-to-noise can be expected for a monopulse system actually designed for deployment in ATRBS. The sources of this improvement are outlined in the following table:

Parameter	TSC	Improved ATRBS	Gain S/N
Antenna Σ Pattern Gain	15.8dB	22 to 24dB	6.2 to 8.2
Cable Loss	4.8dB	3dB	1.8dB
Receiver Diplexer	4.9dB	1.9dB	3dB
TOTAL			11 to 13dB

The antenna used at TSC has a Σ pattern gain of 15.8dB. The beacon monopulse antennas developed under contract to TSC have Σ pattern gains of 22 to 24dB. A 190-foot cable run between the 15th story roof and 11th story laboratory results in a loss of 4.8dB. It should be possible to hold the maximum distance between antenna and transmitter/receiver to just over 100 feet, thereby reducing the loss to 3dB. As previously mentioned the TSC diplexer uses a 3dB hybrid to interface UPX-6 and receiver. In a dedicated system the transmitter can be interfaced with filters, thereby removing this hybrid loss. These three simple improvements result in a 11

to 13dB improvement in signal-to-noise. As a consequence, a system containing these improvements will operate with an expected signal-to-noise ratio of 20dB at the maximum 200 nmi range.

When reply signals are corrupted with additive receiver noise, the measured monopulse off-boresight angle of the received signals is not single valued. The measured angle rather has a probability of falling within certain limits of the actual target azimuth. A measure of the width of this probability distribution is its standard deviation or rms error. An expression for calculating azimuth standard deviation near boresight for a receiver with a wideband IF is given in Table 2.9 of Reference 4:

$$\sigma_{\theta} = \frac{\theta_3}{k_m} \sqrt{\frac{(S/N) + 1}{(S/N)}} \frac{\sqrt{L_{mv}}}{\sqrt{2n B_n \tau}} \quad (4-2)$$

where

- σ_{θ} = standard deviation in azimuth measurement
- θ_3 = half power Σ pattern beamwidth, 4.7°
- k_m = normalized monopulse slope, 1.5
- B_n = IF bandwidth, 11 MHz
- τ = pulse width, $0.45\mu\text{sec}$
- n = number of pulses integrated, $n=1$
- S/N = signal-to-noise ratio, 20dB (100x)
- L_{mv} = system matching loss, 2dB

The system matching loss is principally determined by the video bandwidth-pulsewidth product when the sampling gate is narrow relative to pulsewidth. For a 1.5 MHz video bandwidth and $0.45\mu\text{sec}$ pulsewidth the system matching loss is approximately 2dB (Reference 4, Figure 3.17). In the case of a single reply sampler ($n=1$) the calculated standard deviation for a $S/N=20\text{dB}$ is

$$\sigma_{\theta} = 0.12 \text{ degrees} \quad (4-3)$$

This calculated standard deviation requires modification when a reply originates near the edge of the 3dB sum pattern beamwidth. At the edge of the 3dB sum pattern replies are received at reduced power levels, which leads to an increase in the standard deviation. Figure 9, taken from Figure 2.12 of Reference 4, shows the increase in standard deviation as a function of target off-axis angle for a monopulse system which computes Δ/Σ on a single hit basis. Using this curve it is possible to plot the standard deviation of the receiver as a function of angular offset of a reply from boresight. The solid curve of Figure 10 shows the standard deviation of the log monopulse receiver due to receiver noise alone for a signal to noise ratio of 20 db.

4.2 RECEIVER GAIN MISMATCH

Gain mismatch between the Σ and Δ channels of a log monopulse receiver results in an error in the measurement of the monopulse off-boresight azimuth angle of a received signal. When there is no mismatch between Σ and Δ channels

$$K\theta_T = \frac{\Delta}{\Sigma} \quad (4-4)$$

where

θ_T = the true azimuth offset of a reply

K = monopulse slope

Δ/Σ = error voltage ratio

Equation (4-4) is expressed in decibels by the conversion

$$20 \log K\theta_T = 20 \log \frac{\Delta}{\Sigma} \quad (4-5)$$

If there exists a gain error, δG , between the Σ and Δ channels

$$20 \log K\theta_M = 20 \log \frac{\Delta}{\Sigma} + \delta G \quad (4-6)$$

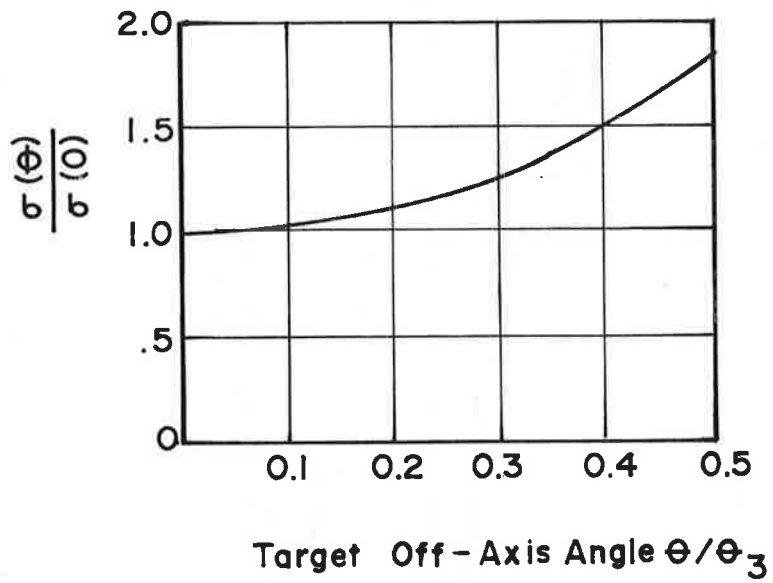


Figure 9. Ratio of Off-Axis Error to On-Axis Error

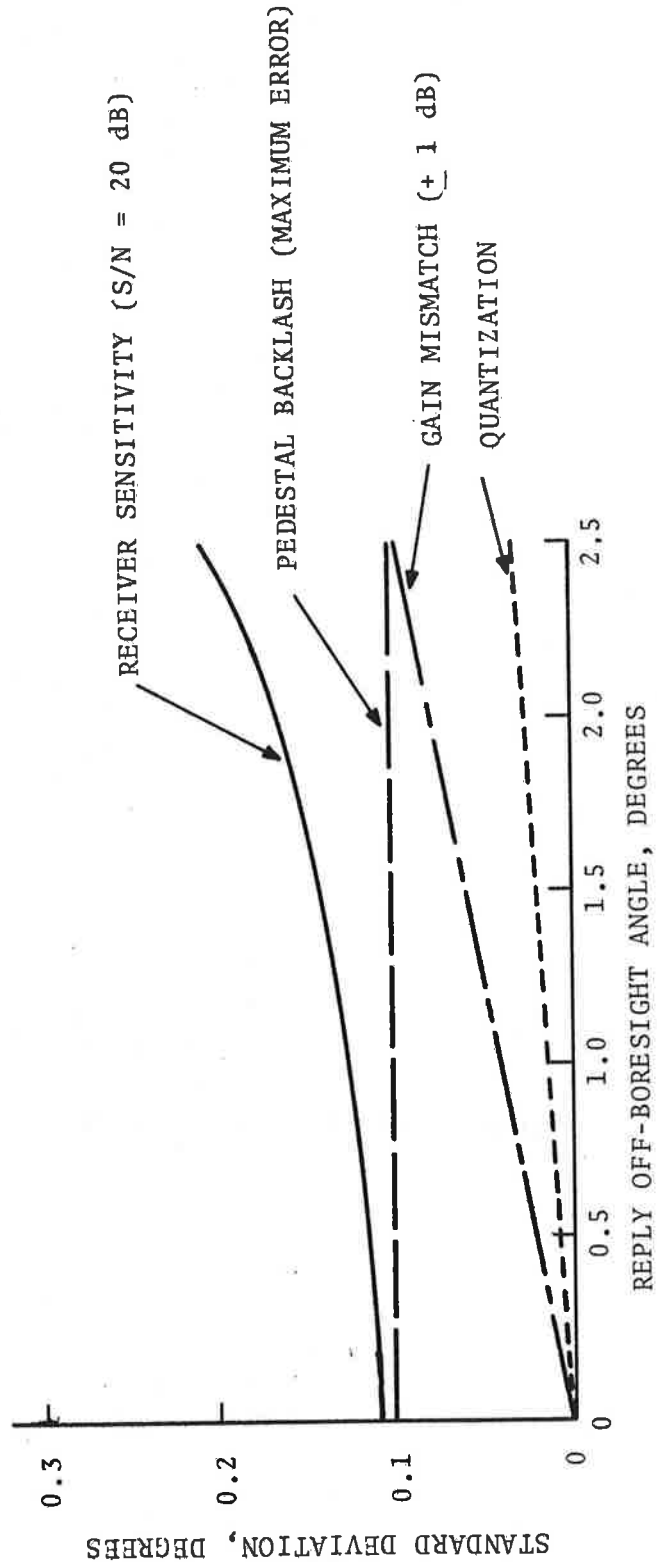


Figure 10. Error Sources in Monopulse Azimuth Measurement

where

θ_M = measured azimuth offset of a reply using a receiver
with channel gain mismatch

δG = gain mismatch in decibels

Substituting eq. (4-5) into (4-6),

$$\log K\theta_M - \log K\theta_T = \frac{\delta G}{20} \quad (4-7)$$

or

$$\log \frac{\theta_M}{\theta_T} = \frac{\delta G}{20} \quad (4-8)$$

To simplify (4-8) the equation is raised to the power 10

$$\frac{\theta_M}{\theta_T} = 10^{\frac{\delta G}{20}} = e^{\frac{\delta G}{8.6}} \quad (4-9)$$

Using the expansion

$$e^x = 1 + x + \frac{x^2}{2!} + \frac{x^3}{3!} + \dots \quad (4-10)$$

Equation (4-9) can be expressed as

$$\theta_M = \theta_T \left[1 + \frac{\delta G}{8.6} + \frac{\delta G^2}{8.6^2 \cdot 2!} + \dots \right] \quad (4-11)$$

For the usual case $\frac{\delta G}{8.6} \ll 1$ eq (4-11) simplifies to

$$\theta_M - \theta_T = \theta_T \cdot \frac{\delta G}{8.6} \quad (4-12)$$

or

$$\delta\theta = \theta_T \frac{\delta G}{8.6} \quad (4-13)$$

where

- $\delta\theta$ = peak error in measured azimuth offset, $\theta_M - \theta_T$
- θ = azimuth offset from boresight at which the measurement is made
- δG = gain mismatch between channels (dB)

Equation (4-13) illustrates that errors due to gain mismatch increase linearly with angle offset of a reply from boresight. Laboratory measurements indicate that the TSC monopulse receiver has a maximum gain mismatch error of 1dB over the dynamic range and reply frequency range. The resultant maximum error for a reply received from 2° off boresight is 0.23 degrees. Figure 10 shows the standard deviation due to gain mismatch in the TSC receiver.

4.3 QUANTIZATION ERRORS

Quantization errors in the single reply sampler result from the operation of the peak detector following the differential amplifier. The peak detector is a 10 bit A to D to A converter operating over a 10 volt input dynamic range. The peak detector generates an analog voltage conforming to its digital memory. The memory holds a level until it is cleared to accept a new sample. The 10 bit converter provides a minimum voltage increment of approximately 10 millivolts. Since the output of a log amplifier is not linear, the minimum angle increment which can be quantized is a function of the offset angle of a reply from boresight. The voltage into the peak detector is

$$V_1 = ak \ 20 \log K\theta \quad (4-14)$$

where

- a = voltage gain due to filter and differential amplifier, 1.13
- k = log amplifier slope, 30mv/dB
- K = monopulse slope, 0.33/degree
- θ = offset azimuth from boresight, degrees

The voltage to the peak detector if the azimuth of the reply is incremented by a small fraction ($\delta\theta$) is

$$V_2 = ak \ 20 \log K(\theta + \delta\theta) \quad (4-15)$$

subtracting V_1 from V_2

$$\frac{V_2 - V_1}{20 \ ak} = \log K(\theta + \delta\theta) - \log K \ \theta \quad (4-16)$$

$$\frac{V_2 - V_1}{20 \ ak} = \log (1 + \delta) \quad (4-17)$$

or

$$10^{\left(\frac{V_2 - V_1}{20 \ ak}\right)} = 1 + \delta \quad (4-18)$$

if the minimum $V_2 - V_1$ is 10 millivolts

$$1 + \delta = 1.0345 \quad (4-19)$$

$$\delta = .0345 \quad (4-20)$$

Therefore, the maximum quantization error expressed in degrees is 0.0345°. For a reply originating at a 2° offset from boresight, the maximum quantization error is 0.069°.

Figure 10 shows the standard deviation due to quantization errors, under the assumption of linear monopulse error slope.

4.4. PEDESTAL SYNCHRO ERRORS

The pedestal used in the TSC monopulse system has a drive system designed for operation with a small millimeter dish antenna. The use of this pedestal to position an antenna 4 feet high and

over 20 feet long results in several problems. Response is sluggish and the gear train has backlash. Depending on the direction of rotation and on wind loading there is a maximum azimuth bias type error due to backlash of ± 0.1 degree. If the antenna is positioned and held under power, the actual boresight is known only to within 0.1 degrees due to wind and static friction in the pedestal. Figure 10 shows the maximum bias error due to backlash.

5. MONOPULSE ACCURACY AT LOW SIGNAL LEVELS

The measured performance of monopulse at low signal-to-receiver-noise ratios was found to be in agreement with the calculations of Section 4.1. To reduce the signal-to-noise ratio, identical attenuators were placed on the Σ and Δ receiver inputs. The attenuators provided a boresight Σ signal 20dB above noise when operating with the fixed transponder at MIT. For these measurements the azimuth of antenna boresight was read from the chart recorder slaved to pedestal position.

The system clock was operated in the single interrogation mode in which the operator initiated one interrogation sequence with a push button. The monopulse signals due to a single interrogation were monitored using two digital voltmeters. One voltmeter displayed the magnitude of the peak detector voltage indicating the magnitude of the angle offset of the reply from boresight. A second voltmeter displayed a positive or negative voltage depending on whether the reply originated from right or left of boresight.

For this experiment the antenna was stopped at 12 different azimuths relative to the fixed transponder. At each of these 12 azimuths the transponder was located within the 3dB beamwidth of the antenna Σ pattern, and at each of the 12 azimuths 20 discrete interrogations of the transponder were made.

The monopulse output voltages were recorded and converted to angle offsets from boresight using a best fit linear approximation to the error curve. The voltage out of the peak detector is given by:

$$V_{\text{out}} = ak 20 \log K\theta \quad (5-1)$$

where

a = voltage gain due to filter and differential amplifier, 1.13

k = log amplifier slope, 30 mv/dB

K = monopulse slope, 0.33/degree

θ = offset azimuth from boresight, degrees

Regrouping the terms in Eq (5-1) and raising it to the power of 10 results in the equation used to convert output voltage to measured offset azimuth angle:

$$\theta = \frac{1}{K} 10^{\left(\frac{V_{out}}{20ak}\right)} \quad (5-2)$$

Figure 11 shows the results of this experiment. The horizontal coordinate is the angular separation between antenna boresight and replying transponder azimuth. The position of the antenna boresight is derived from the slaved chart recorder. The vertical coordinate is the monopulse off-boresight azimuth angle of the received signal. If the chart recorder tracking of antenna position and the monopulse receiver performance were perfect, all measured data would lie along a straight line inclined at 45°. In Section 4.4 the problem of pedestal backlash was mentioned. As a result of backlash, once the antenna is stopped for a measurement set there is an uncertainty of ± 0.1 degree as to the angle at which the antenna is actually pointed. This uncertainty is shown in the figure by plotting a pair of straight lines inclined at 45° and separated by the antenna position reading error. This separation shows the possible error due to pedestal backlash problems. The mean of the 20 point data set is designated by the cross in each set. The extremes of the 20 reply data points at any antenna azimuth is represented by a short dash on the figure. The linearity of the data is good, except near the extremes of the monopulse error curve at $\pm 2^\circ$. The linearity could be improved if the transform to angle used the actual monopulse error curve rather than a best fit linear approximation.

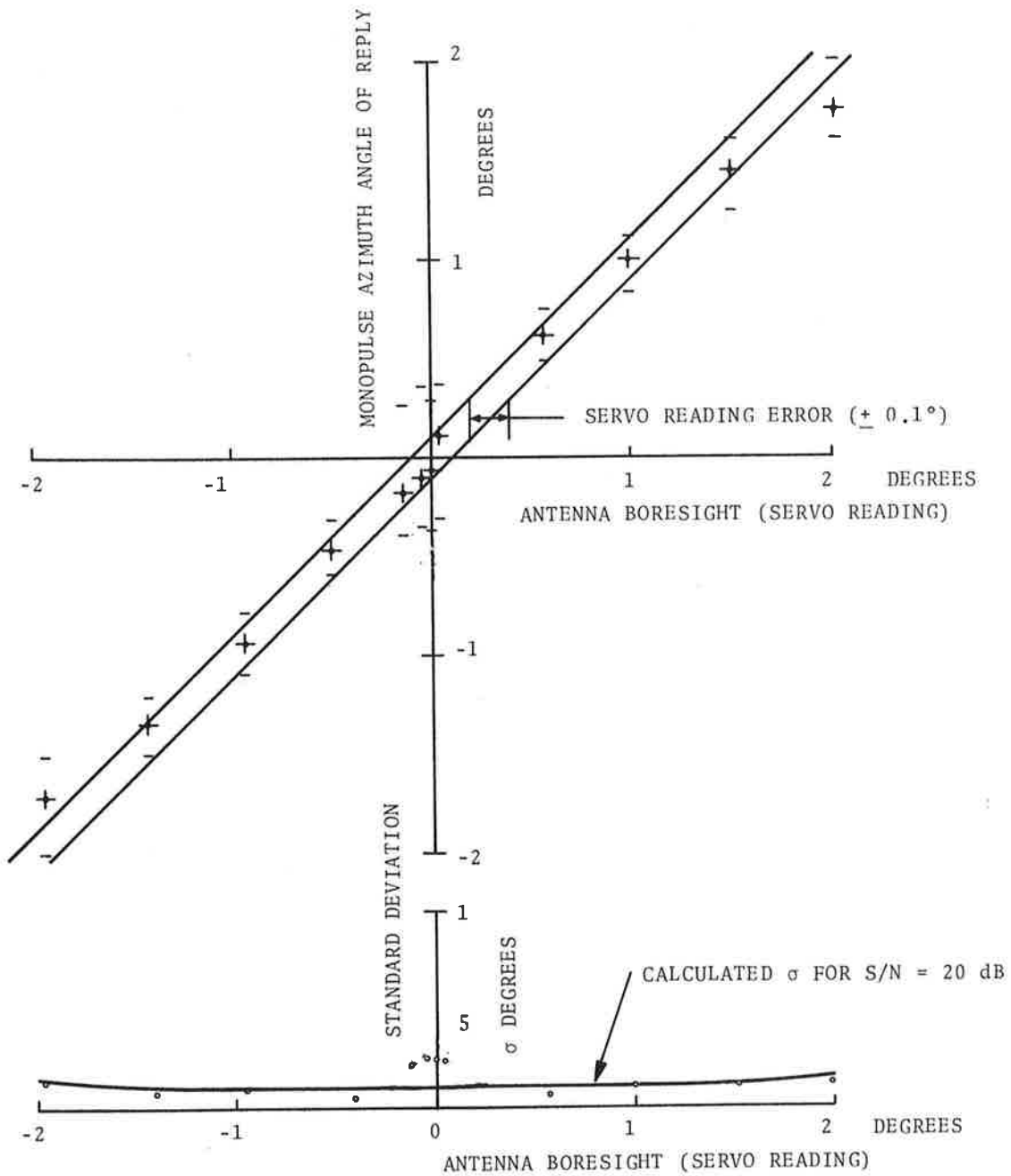


Figure 11. Measured Log Monopulse Receiver Performance, S/N=20dB

Figure 11 also shows the standard deviation of the measured data sets. The solid curve is the value of standard deviation for a S/N of 20 as derived in Section 4.1. The points plotted in the figure are the standard deviation of the 20 point data sets. Comparison shows good agreement between calculations and measurements.

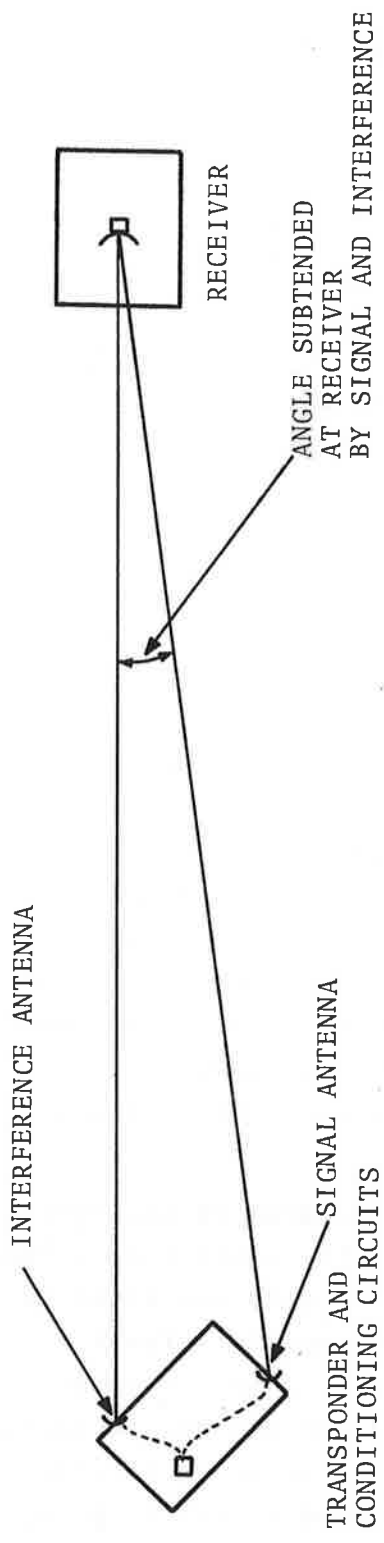
6. MONOPULSE ERRORS DUE TO INTERFERING SIGNALS

In a system which utilizes the monopulse technique for determining target azimuth, the presence of undetected interfering signals due to fruit or signal multipath can result in large measurement errors.⁵ In an effort to evaluate experimentally the magnitude of such errors and to define criteria for identifying the presence of interfering signals a test bed was developed to generate interference at controlled levels and phases. Data accumulated during Fiscal Year 1974 demonstrate the need in any monopulse receiver of a reliable method of detecting the presence of interference for the purpose of flagging and editing such replies.

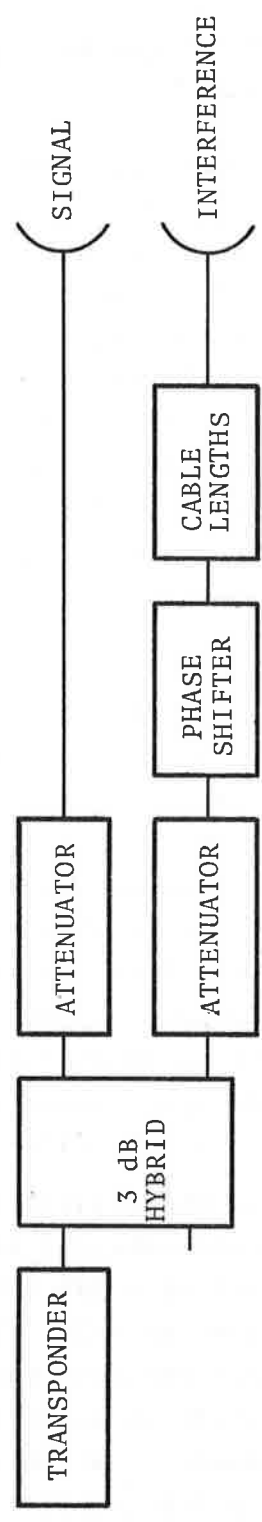
6.1 INTERFERENCE TEST BED

In designing the interference test bed it was considered desirable to be able to vary a number of interference parameters independently. These parameters are the azimuth angle offset between signal and interference, the signal-to-interference power ratio, and the differential phase and timing of the signals and interference. To achieve this degree of flexibility the approach taken was to position two portable horn type antenna sources on the roof of a nearby high rise building. The maximum separation of the antennas on the roof results in an angular separation of 2.6 degrees as viewed from the receiving antenna. A plan view of this setup is shown in Figure 12.

Figure 12 also shows a simplified block diagram of the equipment used to generate coherent interference. The reply from a single transponder is split in a 3dB hybrid. Cable lengths are added to the interference line in order that the signal and interference signals will be received simultaneously. Slight delays between the signals can result in incomplete cancellation of the interfering signals. The attenuators allow the signal to interference ratios to be varied over a 50dB range. Finally, the phase shifter permits the phase between the two transmitting antennas to be varied continuously over 180 degrees.



PLAN VIEW OF INTERFERENCE MEASUREMENTS



GENERATION OF COHERENT INTERFERENCE - BLOCK DIAGRAM

Figure 12. Test Bed for Interference Measurements

6.2 DATA FORMAT

In performing the interference measurements the output of the monopulse receiver was sampled using the boxcar integrator and recorded using the calibrated chart recorder slaved to the antenna azimuth servo. For each value of signal to interference ratio being transmitted a calibration is made. In the calibration, the Σ and the Δ/Σ patterns are recorded with replies transmitted over the antenna at location A only (signal antenna) and subsequently with replies transmitted over the antenna at location B only (interference antenna).

Figure 13 is an example of the recorded data for a S/I of 2.8dB. From these records the value of signal-to-interference at the receiver as a function of azimuth can be directly read. The (Δ/Σ) from the signal antenna provides the receiver calibration curve used in inverting monopulse output voltages to off-boresight azimuth angles. The location of the (Δ/Σ) nulls for both signal and interference locate the azimuth of signal A and interference B on the coordinates of the chart paper.

After the calibration procedure is completed for a particular signal-to-interference ratio both the signal and interference are simultaneously transmitted. Scans by the receiving antenna through the azimuths of the signal A and interference B are made with the phase between A and B equal to 0° , 30° , 60° , 90° , 120° , 150° and 180° . Figures 14 through 17 are the recorded response of the monopulse receiver for signal-to-interference ratios into the transmitting antennas of approximately 2.8dB, 5.6dB, 9.2dB and 15.6dB.

6.3 INTERPRETATION OF RECORDED INTERFERENCE DATA

A monopulse receiver processor translates monopulse output voltage ratio ($\log \Delta/\Sigma$) into off-boresight azimuth angle. Figure 18 shows the manner in which interference produces errors in this translation. On the right side of Figure 18 is depicted a typical set of monopulse output curves corrupted with interference. Only the signal plus interference curves for 0 degrees and 180 degrees phase differential are drawn for the full azimuth range. A small region of the intervening phase differentials are indicated on the

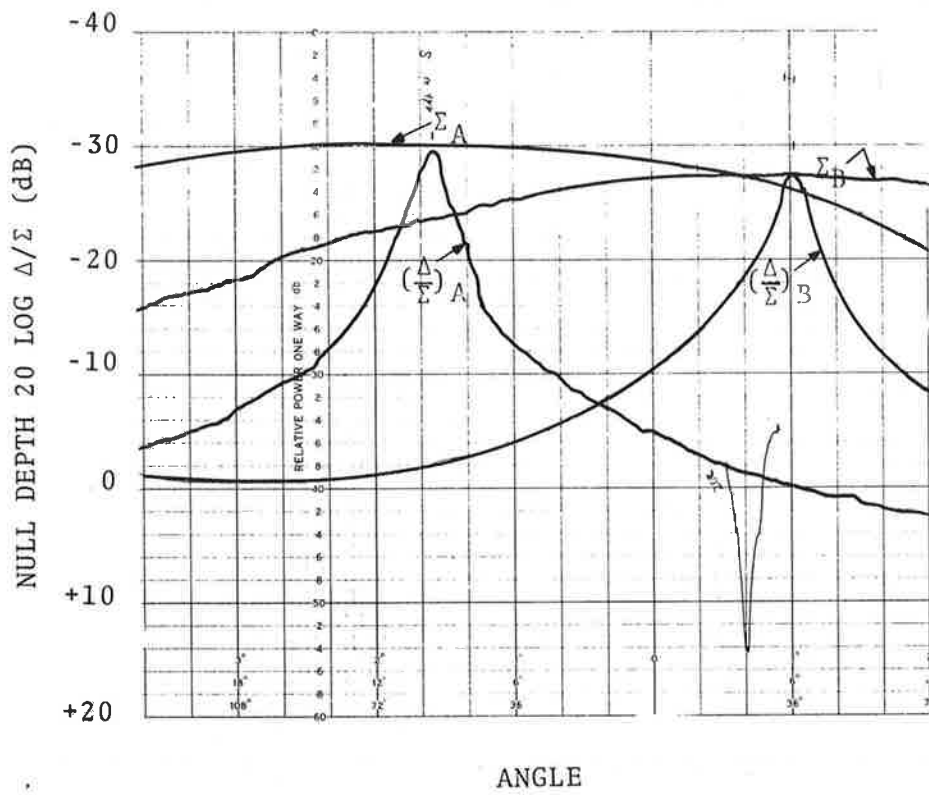


Figure 13. Calibration Curves for $S/I=2.8\text{dB}$

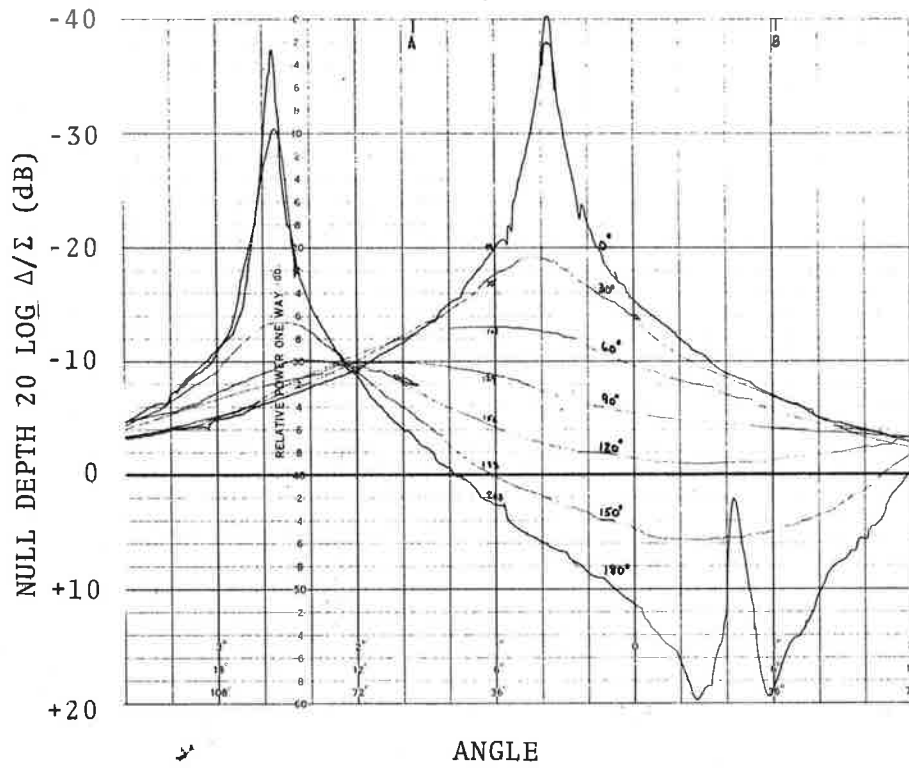


Figure 14. Log Monopulse Response, S/I=2.8dB

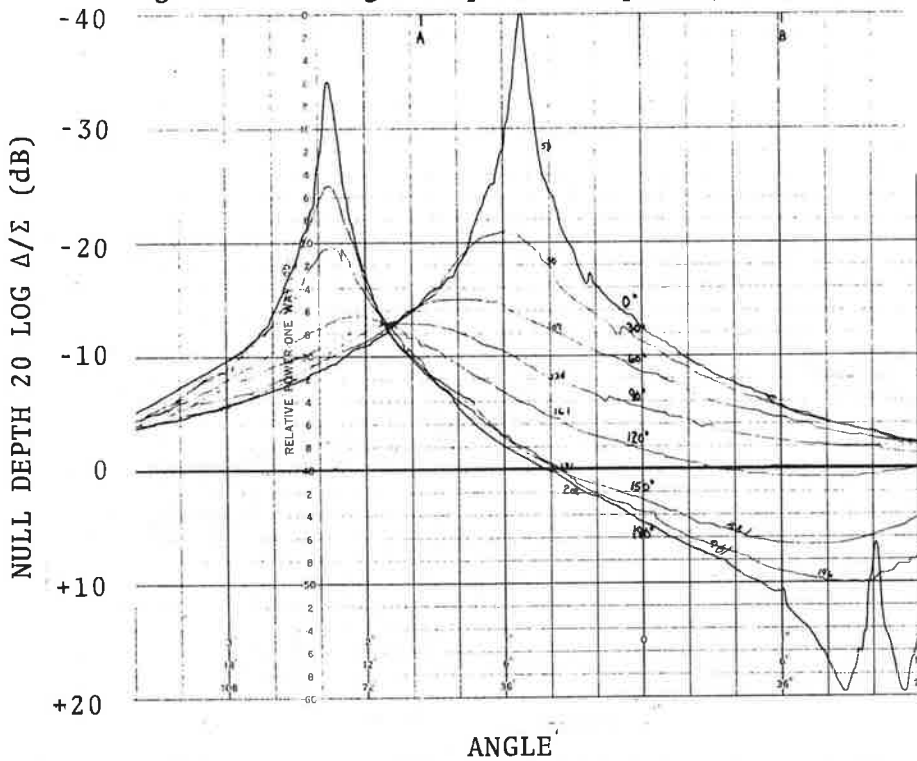


Figure 15. Log Monopulse Response, S/I=5.6dB

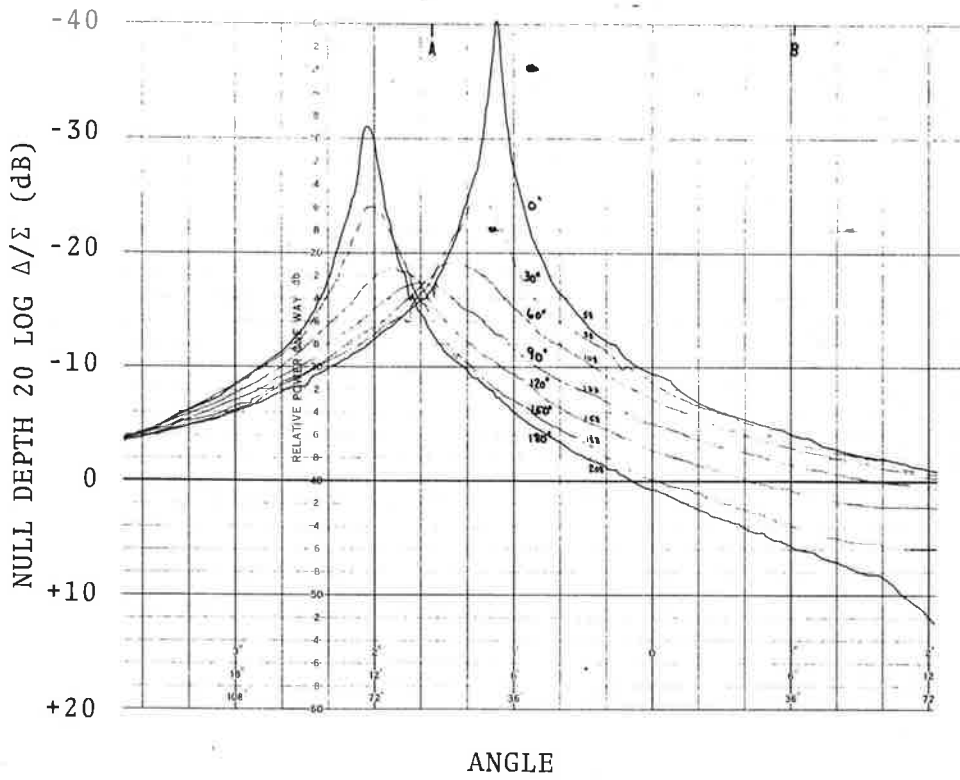


Figure 16. Log Monopulse Response, S/I=9.2dB

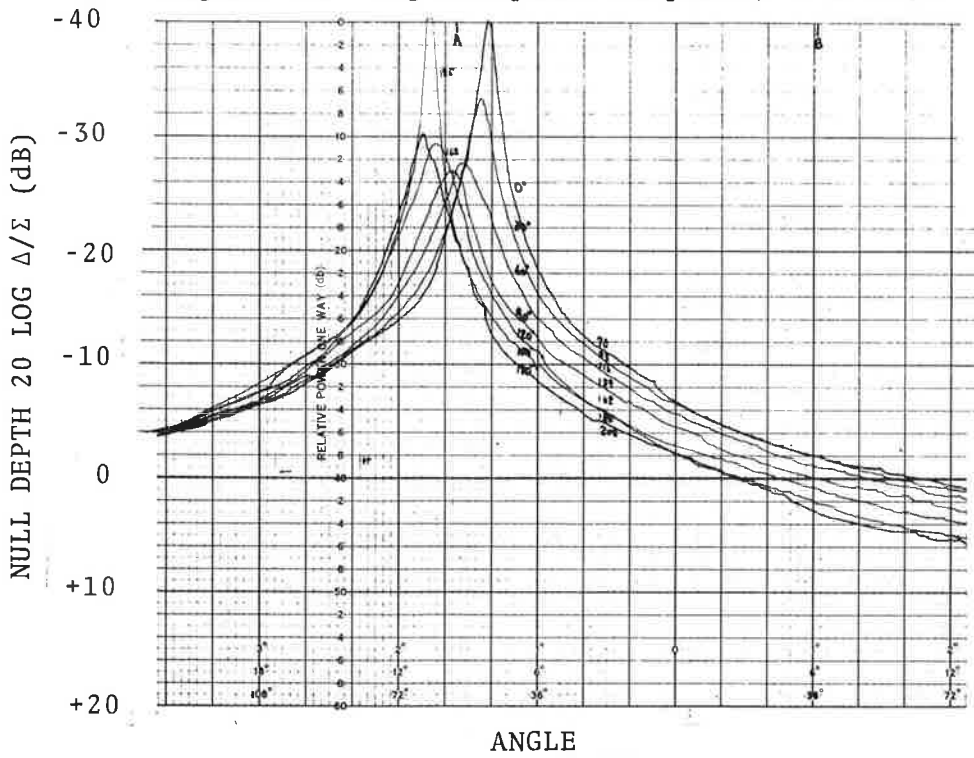


Figure 17. Log Monopulse Response, S/I=15.6dB

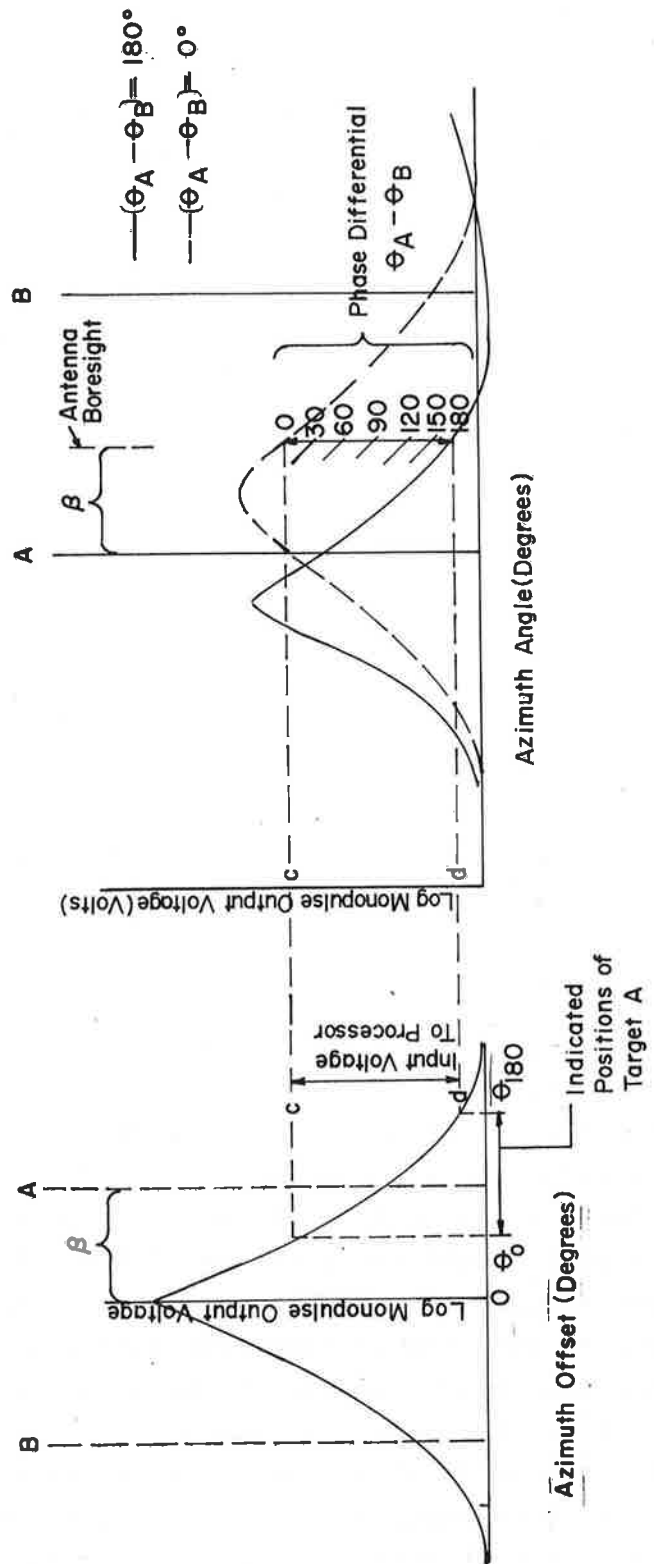


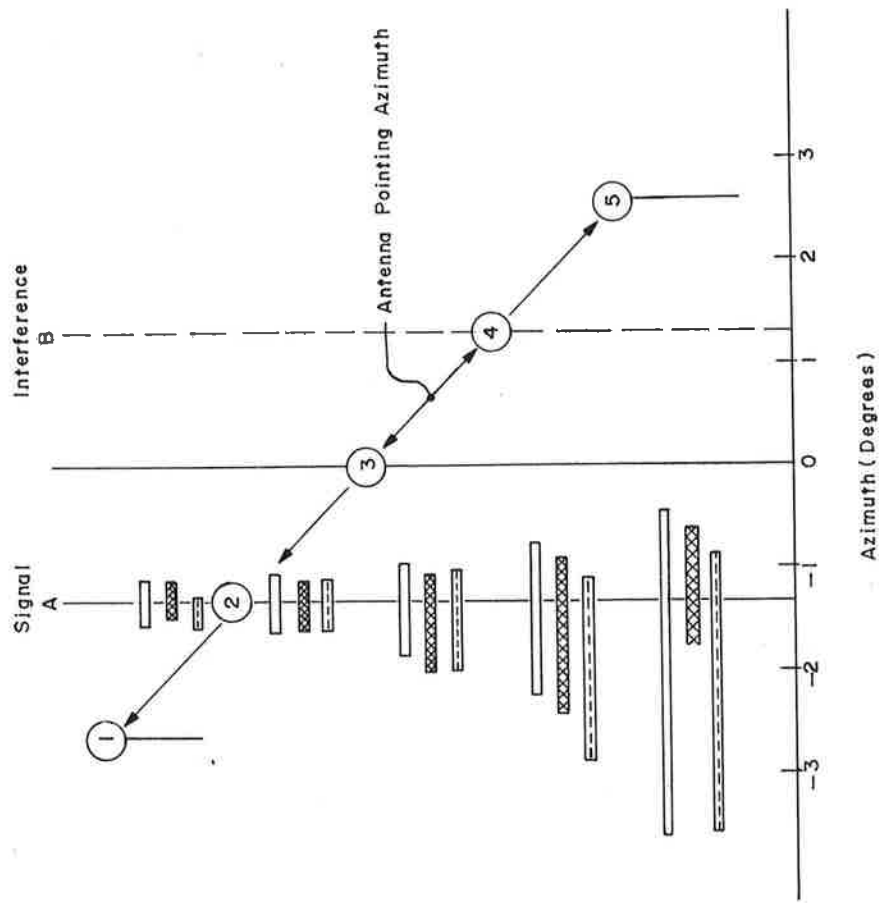
Figure 18. Indicated Target Locations Due to Coherent Interference

figure. Assume that a reply with interference is received when the scanning monopulse antenna boresight is located at an angular offset β to the right of the true target location A. If signal (A) and interference (B) are in phase the output log voltage of the receiver is level c. If the signal and interference have some other phase relationship, the output of the receiver will be a lower voltage, with the minimum (d) occurring when they are 180° out of phase.

On the left side of Figure 18 is the receiver processor translating curve. If voltage levels c through d are translated into azimuth offset by the monopulse processor, the indicated location of the reply can occur anywhere between angles θ_0 and θ_{180} . Angles θ_0 through θ_{180} encompass a large angular region around the true azimuth offset angle A. This spread or uncertainty in the measured azimuth around the true location of A is dependent on the signal-to-interference ratio at the antenna boresight azimuth, β . As the antenna continues to scan, the received signal-to-interference ratio is continuously changing, and hence the uncertainty in predicting the actual location of A is also changing. The technique described for inverting data in this section was used to translate the log voltages recorded in Figures 15, 16 and 17 to azimuth offset angles.

6.4 RESULTS OF INVERTING INTERFERENCE DATA

The monopulse receiver output voltage data recorded for signal-to-interference ratios (S/I) of 15.6, 9.2, and 5.6dB were translated to demonstrate the uncertainty present when measuring the azimuth of a reply under interference conditions. For each of the three S/I conditions a hypothetical monopulse measurement was made at five azimuths evenly spaced around the azimuths of A and B. Figures 19, 20, and 21 show the results of these translations. In these figures the orientation of the antenna boresight with relation to A and B for each of the five monopulse offset measurements is shown by one of the five circled numbers. The extent of the three bars for each antenna orientation shows the possible error in measuring azimuth of the replying transponder located at position A. The three bars are the result of three methods of determining this



Apparent Target Locations Due To Coherent Interference

- ▬ Calculated From S/I
- ▨ Monopulse Error Curve (Actual)
- ▬ Linear Monopulse Error Curve

$(S/I)_{\text{③}} = 15.6 \text{ db}$

Figure 19. Uncertainty in Aircraft Azimuth, S/I=15.6dB

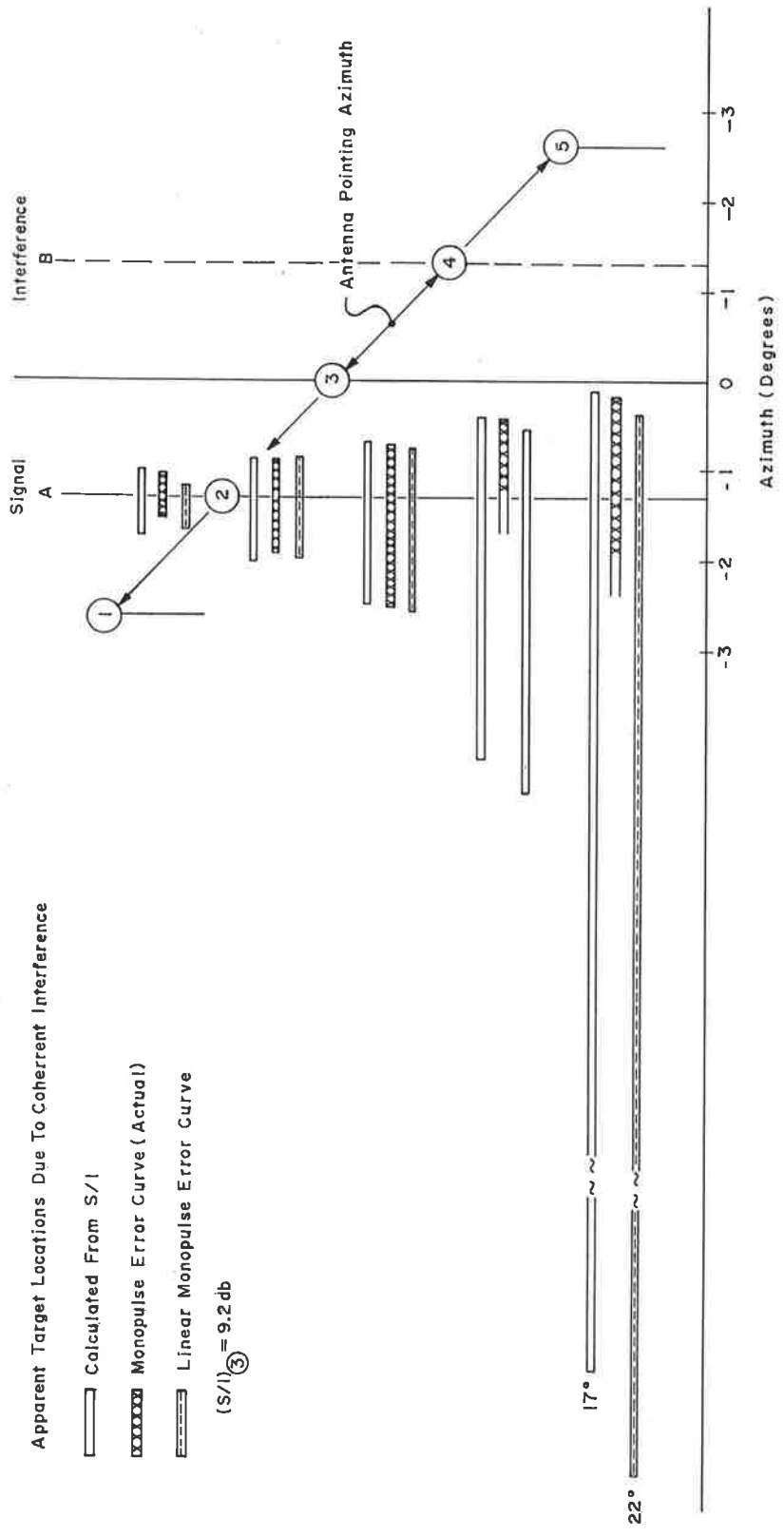


Figure 20. Uncertainty in Aircraft Azimuth, S/I=9.2dB

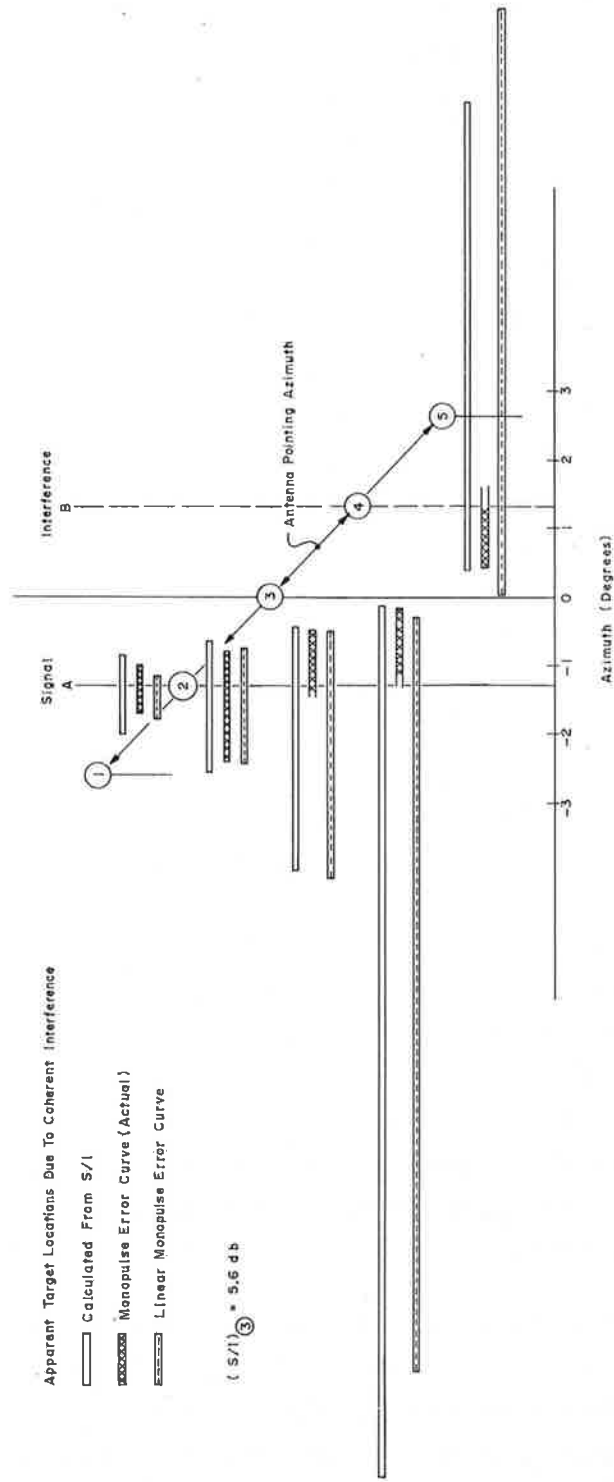


Figure 21. Uncertainty in Aircraft Azimuth, S/I=5.6dB

error. The extremes of the bars correspond to the two cases in which phase between signal and interference is either 0° or 180° . The analysis of Sherman⁵ is applicable to these extremes. The first bar in each set is generated using Sherman's technique, which uses the received S/I ratio vs. azimuth angle recorded as part of the calibration.

The second bar in each set is the azimuth uncertainty, derived by using the actual monopulse error curve for translation, as described in Figure 18. It therefore takes into account monopulse error curve non-linearities. In cases where the indicated voltage exceeds the permissible range by changing polarity ($\Delta/\Sigma > 1$) the actual monopulse error curve cannot provide a transformation. For this reason a third bar is used — a linear approximation to the error curve extending to values of Δ/Σ greater than unity. It is necessary to do this to compare the measured results with the end point analysis. The figures show good agreement between the three methods of determining azimuth over the region for which each is valid.

Figure 19 depicts a case in which the S/I at the two transmitting horn antennas is 15.6dB. The figure shows that the accuracy with which transponder A can be located deteriorates as the antenna axis moves from position 1 through 5. The estimates of A's location made at position 1 are least corrupted because the interference signal enters the antenna from an azimuth at which the antenna power pattern is far down from its peak. Consequently, S/I received is high, yielding small errors. As the antenna scans toward position 5, the power into the antenna due to interference is increased while the power due to the signal is decreased, resulting in a reduced received S/I. As a consequence, the estimate of the location of A is much poorer.

Figure 20 shows the same effect for the case in which S/I into the two horn antennas is 9.2dB. Since the interference is higher, there is an overall increased error in estimating the location of A. Figure 21 shows a case in which S/I into the two horn antennas is 5.6dB. In this case the interference is sufficiently large so that as the antenna scans toward position 5, the receiver locks

on to the interference azimuth as the probable location of the reply. This is expected, because at position 5 and beyond the antenna pattern is such that the received interference exceeds the received signal.

These data demonstrate that even for relatively low levels of interference the errors due to interference exceed those from other sources. As a consequence it is imperative that a receiver be capable of detecting the presence of interference in a return. If one or more replies are received that are tagged as containing interference, it may be best to edit these replies from the scan results. It seems unlikely that the large errors involved can be corrected.

7. RECOMMENDATION FOR FOLLOW-ON EFFORT

It is recommended that the task of characterizing monopulse performance in the air traffic control environment be continued. Specifically, work should be directed toward a direct experimental comparison of the accuracy and reliability of a sliding window processor with a monopulse processor being operated at a reduced prf. Under such a test plan, aircraft would be acquired at Logan Airport at takeoff and followed out to a 100 nautical mile range. During such flights both sliding window centroid data and detailed monopulse centermarking data would be recorded on a scan-by-scan basis. Such data are to be analyzed off-line to provide a comparison of the two techniques and to establish the benefits of beam sharpening RSLs, multiple hit integration, and interference flagging schemes.

As a next step in implementing such a program, a TPX-42 small airport terminal processor has been received and is being made operational. It employs a sliding window processor and will be used in parallel with a monopulse receiver processor for the purpose of conducting measurements of comparative azimuth accuracy.

During Fiscal Year 1974 TSC started the development of a monopulse receiver processor under contract. This receiver uses hard limiters and phase comparators for generating monopulse azimuth offset voltages. The processor will employ a mini-computer permitting maximum flexibility in its operation. Several outstanding capabilities of the monopulse processor are:

1. The monopulse processor will simultaneously track three targets and provide a printout of their azimuths based on monopulse measurements. The printout occurs as each scan is completed to provide a continuing update of target location.
2. The run length or number of monopulse replies processed for target-centermarking can be

varied with instructions to the computer through the teletype keyboard.

3. The processor incorporates variable receiver sidelobe suppression which can be used to edit replies and provide beam sharpening.
4. The receiver incorporates a quadrature channel for detecting and editing signals which contain interference.

In addition to these two major procurements, in-house work has started on building an interface between the TPX-42 Monopulse Processor and a high speed digital recording system. This system will be used to record sliding window centermark on a scan basis and monopulse target estimate, quadrature signal amplitude, and several editing functions on a sweep-by-sweep basis. The data on these tapes will be analyzed in non-real time with varying editing functions to provide the desired one-to-one comparison.

REFERENCES

1. D. R. Rhodes, Introduction to Monopulse, McGraw-Hill, New York, 1959, 119 p.
2. B. Kulke, B. Rubinger, and G. G. Haroules, "Monopulse Azimuth Measurement in ATC Radar Beacon System," Report No. DOT-TSC-FAA-72-6, Transportation Systems Center, December 1971.
3. W. Cohen and C. M. Steinmetz, "Amplitude- and Phase-Sensing Monopulse System Parameters," Microwave Journal, pp. 27-33, October 1959; pp. 33-38, November 1959.
4. D. K. Barton and H. R. Ward, Handbook of Radar Measurement, McGraw-Hill, New York, 1969, pp. 15-47.
5. S. M. Sherman, "Complex Indicated Angles Applied to Unresolved Radar Targets and Multipath," IEEE Trans. Aerospace and Electronic Systems, Vol. AES-7, January 1971.